



Wayne State University

Wayne State University Theses

1-1-2015

Search For Fully Reconstructed W Boson Decay

Sangeetha Baskaran
Wayne State University,

Follow this and additional works at: http://digitalcommons.wayne.edu/oa_theses



Part of the [Elementary Particles and Fields and String Theory Commons](#)

Recommended Citation

Baskaran, Sangeetha, "Search For Fully Reconstructed W Boson Decay" (2015). *Wayne State University Theses*. Paper 415.

This Open Access Thesis is brought to you for free and open access by DigitalCommons@WayneState. It has been accepted for inclusion in Wayne State University Theses by an authorized administrator of DigitalCommons@WayneState.

**SEARCH FOR FULLY RECONSTRUCTED W BOSON
DECAY**

by

SANGEETHA BASKARAN

THESIS

Submitted to the Graduate School

of Wayne State University,

Detroit, Michigan

in partial fulfillment of the requirements

for the degree of

MASTER OF SCIENCE

2015

MAJOR: PHYSICS

Approved By:

Advisor

Date

© COPYRIGHT BY
SANGEETHA BASKARAN

2015

All Rights Reserved

DEDICATION

To my amma, Usha Baskaran and my husband Arvind
Govindaraj.

ACKNOWLEDGMENTS

I want to thank my professor, advisor, Dr. Robert Harr for his kindness, encouragement and inspiration in physics. I am very thankful for all the critical reviews and above all for providing a conducive environment for learning and conducting research.

I want to thank Dr. Ratna Naik, for her continuous support, without which my degree would not be possible. I want to thank Dr. Jogindra Wadehra for first believing in me. I want to thank all the Professors in the physics department, Wayne State, with whom I took classes, who have inspired and supported me.

I want to thank my fellow lab mates, Dillon Fitzgerald, Kevin Siehl and specially Christopher Joseph Clarke for all his help, knowledge sharing and insights.

I want to thank my uncle and aunt, Mohan Sabapathy and Lakshmi Sabapathy for their support and guiding me to Wayne State for my higher studies. I want to thank my friends, Rashmi Bhopi, Deepa Prabhakaran, Vasudha Jain, Launa Asllanaj, Sagar Paudel and all my friends at Wayne State for their support.

I want to thank my parents, Mrs. Usha Baskaran and Mr. Baskaran Natarajan for their support and love. I want to thank them for teaching me the value of education. I want to thank my brother, Mr. Sundara Vadhanan Baskaran for his love and support.

And most importantly, I want to thank my dear husband, Mr. Arvind Govindaraj for being my pillar of strength, for all the sacrifices, for all the love and encouragement, without whom this degree would be impossible.

TABLE OF CONTENTS

Dedication	iii
Acknowledgements	iv
List of Tables	vii
List of Figures.....	viii
Chapter 1 – Introduction	1
1.1. Standard Model.....	1
1.2. W Boson	2
Chapter 2 –Apparatus	4
1.1. Tevatron.....	5
1.2. CDF detector.....	6
1.3. Tracking System	7
1.4. Trigger	8
Chapter 3 –Data Analysis	9
3.1. Computing and Software	9
3.2. Data Processing	9
3.2.1. Analysis Methods	10
3.2.1.1. Background and Signal	11
3.2.1.2. Isolation	12
3.2.1.3. Angle	13
3.2.1.4. Vertex Fitting.....	14

3.3. Particle Reconstruction	15
3.3.1. Pre -Event Selection	15
3.3.2. Event Selection	16
Chapter 4 –Results and Discussion	18
3.4. Pre -Event Selection	18
3.5. Event Selection	29
Chapter 5 –Conclusion	39
Bibliography	41
Abstract	42
Autobiographical Statement	43

LIST OF TABLES

Table 1: Summary of known W^+ decay modes. W^- modes are charge conjugates of the W^+ modes.	3
Table 2: Shows the limit that was used on the properties of the particle to remove the background.	17

LIST OF FIGURES

Figure 2.1: Aerial view of the Fermilab rings. Top ring is the Tevatron, bottom is the Main Injector.....	4
Figure 2.2: Fermilab Accelerator rings.....	5
Figure 2.3: CDF Detector.	6
Figure 2.1: CDF Tracking System.	7
Figure 3.1: Data Processing.	10
Figure 3.2: W boson decay to $D^+ \rightarrow K^- \pi^+ \pi^+$ and $K^{*-} \rightarrow K^+ \pi^-$	11
Figure 3.3: Bottom cone with cone angle, 0.5 radians, contains $D \rightarrow K^- \pi^+ \pi^+$ tracks and Top cone with cone angle, 0.3 radians, contains $K^* \rightarrow K^+ \pi^-$ tracks.....	13
Figure 3.4: “Beam’s eye view” of $D \rightarrow K^- \pi^+ \pi^+$ and $K^* \rightarrow K^+ \pi^-$ decays.	14
Figure 4.1: The distribution is Monte Carlo KPiPi (D) Mass in $2 \text{ GeV}/c^2$. The y-axis is number of events per $2 \text{ MeV}/c^2$	19
Figure 4.2: The distribution is real data, KPiPi (D) Mass in GeV/c^2 . The y-axis is number of events per $2 \text{ MeV}/c^2$	19
Figure 4.3: Distribution is Monte Carlo K^+ from K^* momentum in GeV/c . The y-axis is number of events per $1 \text{ GeV}/c$	20
Figure 4.4: Distribution is real data, K^+ from K^* momentum in GeV/c . The y-axis is number of events per $1 \text{ GeV}/c$	20

Figure 4.5: Distribution is Monte Carlo K^+ from K^* momentum in Z direction in GeV/c. The y-axis is number of events per 2 GeV/c.	21
Figure 4.6: Distribution is real data, K^+ from K^* momentum in Z direction in GeV/c. The y-axis is number of events per 2 GeV/c.....	21
Figure 4.7: Distribution is Monte Carlo π^- momentum in GeV/c. The y-axis is number of events per 1 GeV/c.	22
Figure 4.8: Distribution is real data, π^- momentum in GeV/c. The y-axis is number of events per 1 GeV/c.....	22
Figure 4.9: Distribution is Monte Carlo $K\pi(K^*)$ mass in GeV/c ² . The y-axis is number of events per 5 MeV.....	23
Figure 4.10: Distribution is real data, $K\pi(K^*)$ mass in GeV/c ² . The y-axis is number of events per 5 MeV.....	23
Figure 4.11: Distribution is Monte Carlo $K\pi(K^*)$ momentum in GeV/c. The y-axis is number of events per 1 GeV/c	24
Figure 4.12: Distribution is real data, $K\pi(K^*)$ momentum in GeV/c. The y-axis is number of events per 1 GeV/c	24
Figure 4.13: Distribution is Monte Carlo $K\pi(K^*)$ momentum in z direction in GeV/c. The y-axis is number of events per 4 GeV/c.....	25
Figure 4.14: Distribution is real data, $K\pi(K^*)$ momentum in z direction in GeV/c. The y-axis is number of events per 4 GeV/c.....	25

Figure 4.15: Distribution is Monte Carlo W mass GeV/c^2 . The y-axis is number of events per $2 \text{ GeV}/c^2$	26
Figure 4.16: Distribution is real data W mass GeV/c^2 . The y-axis is number of events per $2 \text{ GeV}/c^2$	26
Figure 4.17: Distribution is Monte Carlo W momentum in GeV/c . The y-axis is number of events per $1 \text{ GeV}/c$	27
Figure 4.18: Distribution is real data W momentum in GeV/c . The y-axis is number of events per $1 \text{ GeV}/c$	27
Figure 4.19: Distribution is Monte Carlo, Vertex Fitted K^* mass in GeV/c^2 . The y-axis is number of events per 8 MeV	28
Figure 4.20: Distribution is real data, Vertex Fitted K^* mass in GeV/c^2 . The y-axis is number of events per 8 MeV	28
Figure 4.21: Distribution is Monte Carlo $K\text{PiPi}$ (D^+) isolation. Y axis is the number of events per 5 units. Vertical line on the plot is the cut made in the selection process in the step 2.	30
Figure 4.22: Distribution is real data $K\text{PiPi}$ (D^+) isolation. Y axis is the number of events per 5 units. Vertical line on the plot is the cut made in the selection process in the step 2	31
Figure 4.23: Distribution is Monte Carlo K^* isolation. Y axis is the number of events per 5 units. Vertical line on the plot is the cut made in the selection process in the step 2.	32

Figure 4.24: Distribution is real data K^* isolation. Y axis is the number of events per 5 units. Vertical line on the plot is the cut made in the selection process in the step 2	33
Figure 4.25: Distribution is Monte Carlo $K\pi\pi$ (D^+) Mass. Y axis is the number of events per $2 \text{ MeV}/c^2$. Vertical line on the plot is the cut made in the selection process in the step 2.	34
Figure 4.26: Distribution is real data $K\pi\pi$ (D^+) Mass. Y axis is the number of events per $2 \text{ MeV}/c^2$. Vertical line on the plot is the cut made in the selection process in the step 2....	35
Figure 4.27: Distribution is Monte Carlo K^* mass in GeV/c^2 after selection. The y-axis is number of events per $5 \text{ MeV}/c^2$	36
Figure 4.28: Distribution is real data, K^* mass in GeV/c^2 after selection. The y-axis is number of events per $5 \text{ MeV}/c^2$	36
Figure 4.29: Distribution is Monte Carlo, W mass in GeV/c^2 after selection. The y-axis is number of events per $2 \text{ GeV}/c^2$	37
Figure 4.30: Distribution is real data, K^* mass in GeV/c^2 after selection. The y-axis is number of events per $2 \text{ GeV}/c^2$	37
Figure 4.31: 3D Distribution is real data, $K\pi\pi$ mass and W Mass in GeV/c^2 after selection.	38
Figure 5.1: Exponential fit of W Mass.	39

CHAPTER 1 – INTRODUCTION

1.1 STANDARD MODEL

In standard model, matter, also called fermions are classified as quarks and leptons. Quarks are of 6 types divided into 3 generations. Particles belonging to the first generation are more stable and particles belonging to second and third generation is unstable. Up and down quarks make up the first generation, charm and strange quarks make up the second generation, and top and bottom quark make up the third generation.

Leptons are also divided into 3 generations. Electron neutrino and electron are of the first generation, μ neutrino and μ make up the second generation, and τ neutrino and τ make up the third generation. All neutrinos are electrically neutral, but electrons, μ and τ have an electric charge.

There are 4 fundamental forces, 1. Strong force. 2. Electromagnetic force. 3. Weak force. 4. Gravitational force. The strong and weak force acts only over a short distance, at the subatomic level and Electromagnetic and gravity force have infinite range. In the standard model, these forces act due to the exchange of particles called “bosons” named after Satyendra Bose. There are 5 types of bosons in the standard model. Gluons are responsible for the strong force; W and Z bosons are responsible for the weak force; photons are responsible for the electromagnetic force; and gravitons are predicted to be responsible for the gravitational force [1].

Various decay modes of Z and W boson have been observed and their branching fractions measured. For the Z boson, there are over 55 decay modes measured [11]. But for the W boson, there are just 10 decay modes observed so far.

One of the decay modes of the Z boson to note is, $Z \rightarrow D^\pm X$, whose branching fraction is $(12.2 \pm 1.7) \%$ as this is similar to the W decay sought in this analysis. The quark level decay mode of the W boson, $W \rightarrow c\bar{s}$, has branching fraction $31^{+13}_{-11} \%$ [11]. This decay mode can hadronize to the signal for mode $W \rightarrow D^\pm K^*$.

1.2 W BOSON

The W boson was introduced as part of the unification of the weak and electromagnetic interactions in the 1960's [1]. The W boson was observed in 1982 by the UA1 and UA2 experiments at the CERN Super Proton-Antiproton Synchrotron Collider. The following were observed in these experiments:-

1. Observed decays are $W \rightarrow e^+ \nu_e$ and $W \rightarrow \mu^+ \nu_\mu$, where neutrino is inferred from missing transverse energy (MET).
2. Lepton plus MET is established as the commonly used signature of a W boson.
3. Required detector with close to 4π coverage to measured MET.

W boson, so far has been observed to have following decay modes with their branching fraction as follows in Table 1 [11],

Decay Mode	Branching Fractions	Confidence Level
$l^+ \nu$	[a] (10.80 ± 0.09) %	
$e^+ \nu_e$	(10.75 ± 0.13) %	
$\mu^+ \nu_\mu$	(10.57 ± 0.15) %	
$\tau^+ \nu_\tau$	(11.25 ± 0.20) %	
Hadrons	(67.60 ± 0.27)%	
$\pi^+ \gamma$	$< 8 \times 10^{-5}$	95%
$D_s^+ \gamma$	$< 1.3 \times 10^{-3}$	95%
cX	(33.4 ± 2.6) %	
$c\bar{s}$	(31^{+13}_{-11}) %	
invisible	[b](1.4 ± 2.8) %	
[a] l indicates each type of lepton (e, μ , and τ), not sum over them.		
[b] This represents the width for the decay of the W boson into a charged particle with momentum below detectability, $p < 200\text{MeV}$.		

Table 1: Summary of known W^+ decay modes. W^- modes are charge conjugates of the W^+ modes[11].

About 10^7 W bosons are produced at the Tevatron (Run II) and about 10^8 at LHC (Run I). And still there are no observations of an exclusive hadronic W decays.

The W boson, electrically charged weak force carrier is responsible for β decays. Together with the Z boson, it carries the weak force. From the time of its discovery in 1983, there have been various measurements of the W boson mass. Combining the results from the Tevatron and e^+e^- LEP colliders, the W mass is measured to be, $80.385 \pm 0.015 \text{ GeV}/c^2$ and a W width is $2.085 \pm 0.042 \text{ GeV}/c^2$ [3].

CHAPTER 2 - APPARATUS

At Fermilab, proton and anti-proton beams are accelerated to 980 GeV and made to collide at the center of mass energy of 1960 GeV. The W boson is produced when an up quark of a proton and an anti-down quark of an anti-proton hard scatter when collided. To do this, various components go into producing, accelerating, colliding, detecting and depositing the beams and particles.

The Fermi National Accelerator Laboratory was founded in 1967 near Batavia, Illinois, United States. The Fermilab accelerators are located on a 6800-acre site (see Figure 2.1) [5]. For over 25 years until September 2011, the Tevatron accelerator was in operation, smashing protons and antiprotons. Fermilab and its associated groups continue to investigate the data [4].



Figure 2.1: Aerial view of the Fermilab rings. Top ring is the Tevatron, bottom is the Main Injector

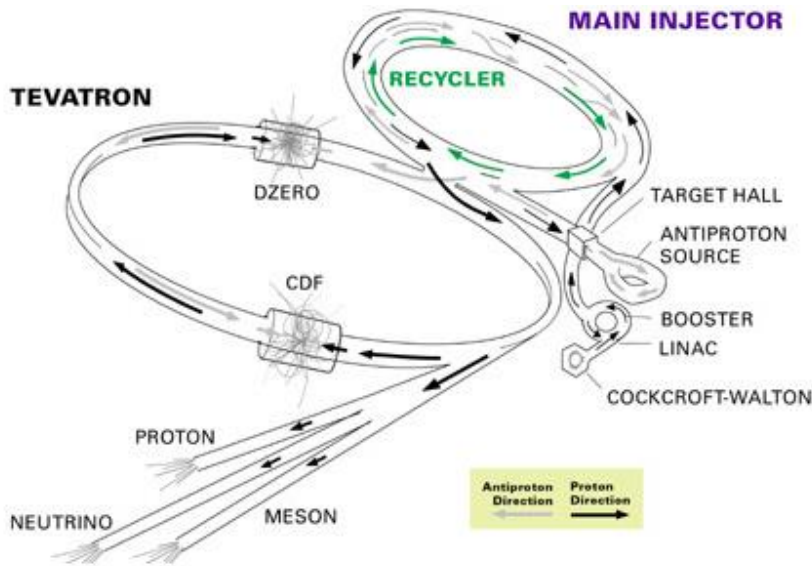


Figure 2.2: Fermilab Accelerator rings

2.1 TEVATRON

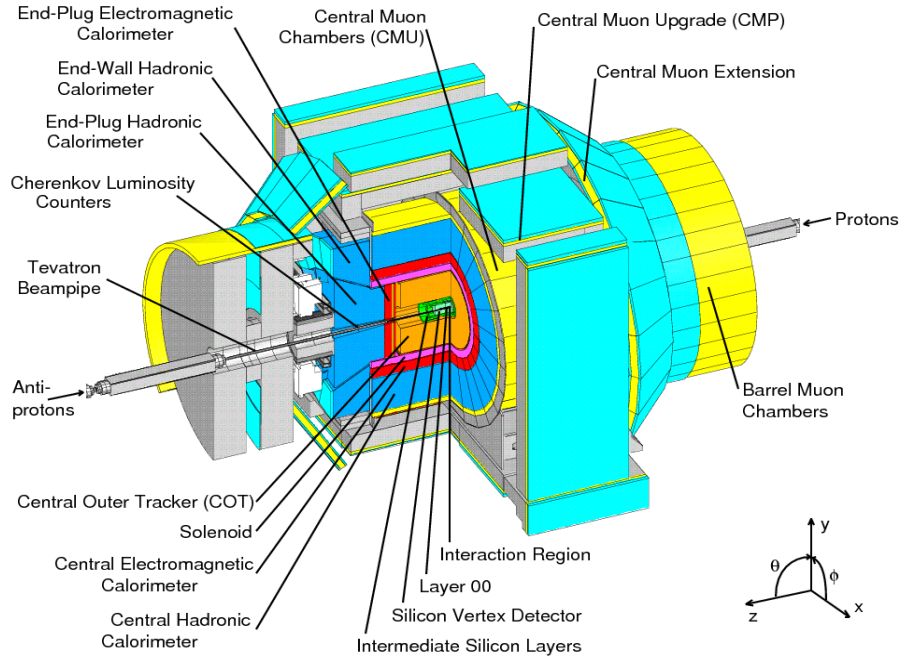
The Tevatron (see Figure 2.2) beams begin where hydrogen gas is converted to hydrogen ions, H^+ , and accelerated in a linear accelerator (Linac). The main purpose of the Linac is to increase the energy of the negatively charged H ion beam from 750 KeV to 400 MeV. From the Linac, the beam gets transferred to the Booster, which removes the electrons from the ions, leaving only the protons. The protons are accelerated to 8 GeV and sent to the Main Injector. The Main Injector accelerates the protons and anti-protons from 8 GeV to 150 GeV and sends beams of 150 GeV protons or anti-protons to the Tevatron [6]

The Tevatron accelerator, is a superconducting magnet synchrotron located in a circular tunnel of radius 1 km. It contains a series of guiding dipole magnets, super cooled to 4.6K. The magnets, when cooled to such low temperatures, become superconducting.

The magnets guide the beams loaded with protons and antiprotons. The 150 GeV protons and anti-protons are accelerated to 980 GeV and made to collide at the CDF and D0 detectors. The data of this research come from the collisions recorded by CDF detector.

2.2 CDF DETECTOR

The CDF Detector (see Figure 2.3) at the Fermilab Tevatron was in operation from 1985 to 1995 (Run I) and 2000 to 2012 (Run II). In this work, we have used data that was gathered by the upgraded detector in Run II. Here we give a brief description of the CDF Run II detector. There are several components that go into this detector and we will discuss



the ones relevant to this work [7].

Figure 2.3: CDF Detector

A Spherical Coordinate system around the beam axis is used to locate a particle as shown in the right bottom corner of Figure 2.3. The polar angle θ is measured from the proton beam axis and azimuthal angle ϕ from the plane of the Tevatron. The pseudo-rapidity is,

$$\eta = -\ln(\tan \frac{\theta}{2}) \dots\dots\dots \text{Equation 1.}$$

2.3 TRACKING SYSTEM

The Tracking system [8] is placed inside a superconducting solenoid of radius 1.5 m and length 4.8 m. The solenoid generates a 1.4 T magnetic field, parallel to the proton-antiproton beam (z) axis. Important components of this system are discussed.

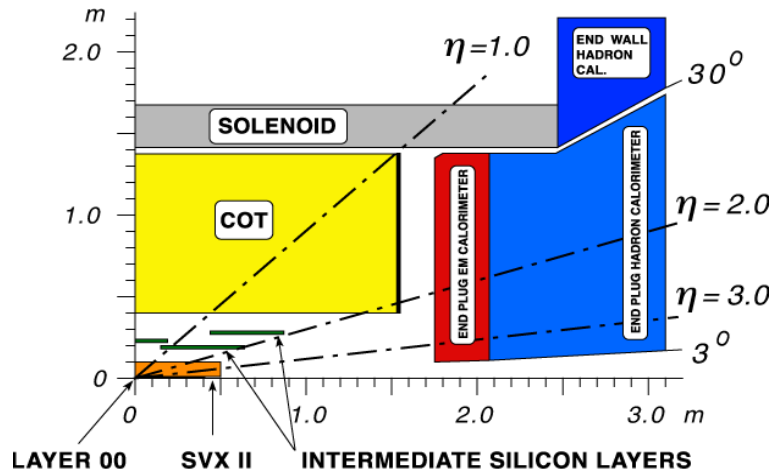


Figure 2.4: CDF Tracking System

The Central Outer Tracker (COT) (see Figure 2.4), measures the tracks of charged particles. It has a radial coverage from 44 to 132 cm and pseudo-rapidity in the region, $|\eta| \leq 1$. The COT measures the momentum of the charged particle track, the angle of bending, and the position of the tracks.

In the CDF silicon system, there are 3 main layers: (1) Layer 00; (2) Silicon Vertex Detector (SVX II); and (3) Intermediate Silicon Layers (ISL).

The SVX has a total of 6 layers. The ISL silicon layer is placed at a radius of 22cm. These layers accurately measure the positions of the charged particles. They also can accurately measure if the track comes from the non - collision vertex. They cover pseudo-rapidity in the region, $|\eta| \sim 2$. The SVX is used to detect secondary vertices

2.4 TRIGGER

There are over a million collisions in the CDF detector per second. It is important that only desired events are selected for the effective analysis of physics. To do this, CDF has a system of hardware and software to catch only those events that have useful characteristics. The trigger system contains 3 levels of operations (Level1, Level2, and Level 3). At each level events are filtered by various components. Level 1 and 2 are mostly hardware based and Level 3 is based on software algorithms. Here we will discuss Silicon vertex trigger at Level 2, whose selected events are what we have used in the search [7].

2.4.1 SILICON VERTEX TRIGGER (SVT)

The SVT uses hit information readout from SVX to compute if an event is likely to contain a secondary vertex. The SVT selects decays of charm and bottom hadrons. This is possible because of the ability of SVT to trigger on vertices with 2 displaced tracks [7].

Chapter 3 – DATA ANALYSIS

3.1 COMPUTING AND SOFTWARE

The CDF production runs on Linux farms, and the computing environment is the Linux operating systems. Large data volumes of around 250 Terabytes are stored on tapes, operated by robots and controlled by Hierarchical Storage Management software. A database system is used to control the access to these datasets.

We submitted the event data request to these databases by giving the specification of the dataset and criteria for event selection [9].

3.2 DATA PROCESSING

The overall picture of how the raw data from the detector processes for event selection is shown in the Figure 3.1. The raw data output from the detector is written on tapes. Then, the reconstruction programs use this raw data as input and reconstructs into physics objects like tracks, electrons and jets. The reconstructed events are then written to tape. In the second step, the reconstructed data are processed and higher level objects are reconstructed and saved. The higher-level objects are analysis specific. In our case, they are bottom and charm hadron candidates stored in a format called Bstntuple. These reconstructed events are available to users as Bstntuple datasets for analysis.

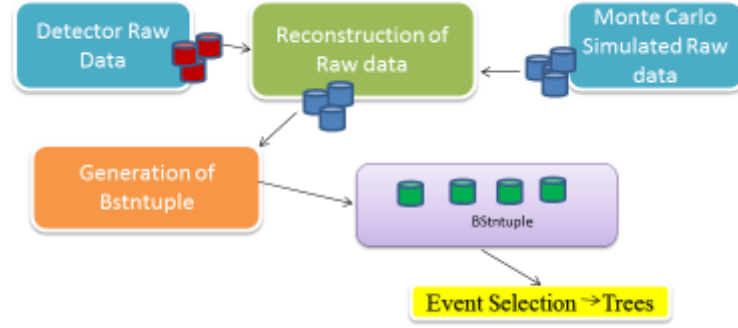


Figure 3.1: Data Processing

We use Monte Carlo program to simulate the $W \rightarrow D^\pm K^*$ decays in order to estimate the efficiency of the trigger, reconstruction and selection. Monte Carlo is a set of computer algorithms that creates simulated events based on the current understanding of the standard model and a detailed simulation of the detector response. The W production is simulated with PYTHIA, the decay with EVTGEN, and the detector with GEANT.

3.2.1 ANALYSIS METHODS

We used CDF Run II data taken between the years 2003 to 2011 for the analysis. We coded in C++ using the CDF software within the Root framework to select events processed into Bstntuples, for both real and Monte Carlo simulated data. If the selections on Monte Carlo simulated events correctly gave a satisfying reconstruction of D^\pm and expected K^* mesons, then we ran the same code on the real data.

We made the selection process in 2 steps; in the first step, which is called Pre-Selection, we used the CDF grid to run a selection algorithm on BStNtuplized data and got the results in the form of trees and in the second step, which is called Selection, we did selection on the events from first step to further optimize the signal.

Figure 3.2, shows the Feynman diagram for a W boson decaying into 2 daughter particles, D and K^* . The D meson decay from the W boson is reconstructed in the $K^-\pi^+\pi^+$ decay mode and stored in the Bstntuples. In our code, we just retrieved the D meson details.

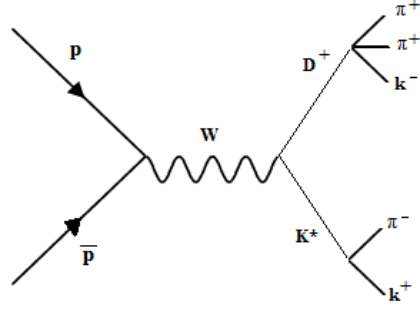


Figure 3.2: W boson decay to $D^+ \rightarrow K^- \pi^+ \pi^+$ and $K^* \rightarrow K^+ \pi^-$

3.2.2 BACKGROUND AND SIGNAL

An important step in the analysis is identifying the right signal. The purpose of this search is to identify a particular decay of the W boson as shown in the Figure 6. Initially the signal has lots of background which is contributed by various phenomena. We apply selection requirements to optimize the signal to background.

For this analysis, any signal other than W boson and its decay products are considered background. We used Monte Carlo simulated data to estimate the efficiency for signal. The data, outside of a signal mass window, can be considered as being all backgrounds. We made the selection process in 2 steps.

In the first step, Pre-Selection, our main methods of identifying the signal was based on filtering the events based on mass, momentum, isolation variables and angle with the beam axis.

In the second step, Selection, we used D^+ mass and D^+ and K^* Isolations to further remove the background.

Here, we will discuss some of the event selection methods in detail.

3.2.3 ISOLATION

We used Isolation to do selection on the events. Isolation, I is calculated by the following equation,

$$I = \frac{|\vec{P}_{D^+}|}{\sum \vec{P}_\pi} \dots \dots \dots \text{Equation 2.}$$

\vec{P}_{D^+} , Momentum of D^+ . $\sum \vec{P}_\pi$, Total momentum of all tracks within the cone angle.

We used the isolation variable because a D^+ or K^* from a W decay will not come with additional particles. But if the D^+ or K^* come from standard interactions, then there is a high probability that other particles will be nearby. This happens because the other processes usually involve the fragmentation of quarks, and this tends to produce lots of other particles nearby (that is, within the chosen cone) of the high momentum D^+ or K^* . So, asking that there NOT be other particles nearby helps to separate signal from background. To do this, we used the cone angle to isolate the tracks and calculated the total momentum, $\sum \vec{P}_\pi$, of all the tracks within the cone angle. Figure 3.3, shows the kaon (K) and pion (π) tracks decaying from D^+ and K^* .

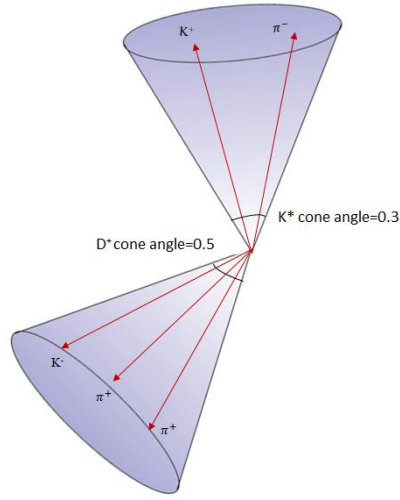


Figure 3.3: Bottom cone with cone angle, 0.5 radians, contains $D \rightarrow K^- \pi^+ \pi^+$ tracks and Top cone with cone angle, 0.3 radians, contains $K^* \rightarrow K^+ \pi^-$ tracks

3.2.4 ANGLE

Figure 3.4, shows the tracks of $D \rightarrow K^- \pi^+ \pi^+$ and $K^* \rightarrow K^+ \pi^-$. To form K^* candidate, we have to select kaons (K^-) and pions (π^+) that decayed from K^* particle. We used the angle that K^- and π^+ tracks make with the D^+ candidate to form K^* and reduce background.

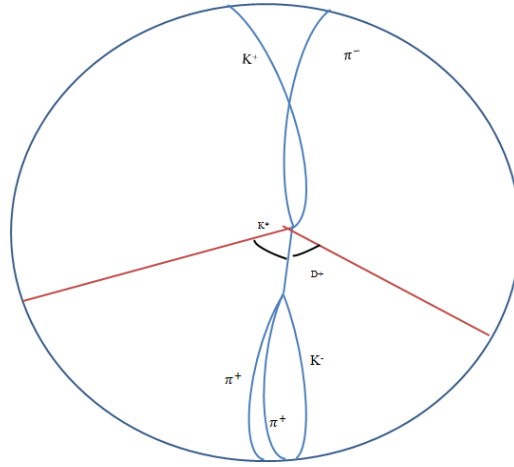


Figure 3.4: "Beam's eye view" of $D \rightarrow K^- \pi^+ \pi^+$ and $K^* \rightarrow K^+ \pi^-$ decays

3.2.5 VERTEX FITTING

The K^* that decays from W , will immediately decay into K^+ and π^- daughter particles. Whereas the D^+ will travel some distance before decaying into the K^- and $2 \pi^+$. The position where a particle decays are called Vertex and the vertex information for the tracks are detected and stored in the Bstntuple. To reduce the background due to K^* , that is not part of the decay mode of this analysis, we can use vertex information of K^* . In this analysis, we have not selected events based on Vertex information of K^* but we did vertex fitting and stored information of vertex fitted K^* Mass, L_{xy} , L_{xy} error, chi square, distance in z direction for future analysis.

3.3 PARTICLE RECONSTRUCTION

3.3.1 PRE-SELECTION

In our code, we start with the D^+ candidates that have been already identified from the tracks and saved in the Bstntuple. The already reconstructed D meson is of the form $D \rightarrow K^- \pi^+ \pi^+$. The properties of the D^+ , K^- , π^+ , π^+ are saved in a tree. We discard the D candidates with transverse momentum P_T less than 15.0 GeV/c or with mass error is greater than 0.05 GeV/c². We calculated the charged track isolation of the D^+ candidates as shown in equation 2. If isolation is less than 0.75, we discard the D.

Next, we formed K^{*0} candidate. The K^{*0} candidate is a decay child of W boson will decay to, $K^* \rightarrow K^+ \pi^-$, 50% of the time. We have used various selection criteria for pion and kaon of a K^* candidate.

We first select kaons and pions of K^* from the list of kaon and pion tracks by its charge. The pions will have charge opposite to the D candidate, selected in a particular event, therefore we use pion track that has the opposite charge of the D candidate. We further filter the pion tracks using the transverse momentum P_T . We discard those pion tracks whose momentum are less than 5.0 GeV/c. The kaon will have the same charge as the D candidate selected in a particular event.

Next, we select the kaons and pions of K^* candidates by the angle it makes with the D candidate. We use only the tracks that lie more than $\pi/6$ radians from the D^+ .

Next, we combined the selected kaon and pion tracks of K^* candidates and calculated it's mass. We selected only those K^* candidates whose mass are less than 1.096

GeV. We then combined the selected K^* and D^+ candidates to form a W candidate. We discarded those W candidates whose mass are less than 40 GeV.

Next we calculated the Isolation value for K^* candidate using the equation 2. At pre-selection, we require the K^* isolation to be greater than 0.75.

By doing these event selections, we were able to discard lots of background signal. All the properties of the pions, kaons, reconstructed K^* and Ws are stored in the tree.

From the selected pions and kaons of K^* , we did vertex fitting of pion and kaon tracks and calculated the K^* mass, L_{xy} , L_{xy} error, chi square, distance in z direction from the combined track.

3.3.2 SELECTION

With the tree file from the pre-selection step as input, we further did the event selection to remove more background. We first selected events by setting limits on values like momentum of K^* , D^+ , kaon, pion, L_{xy} value of D^+ , vertex fitted mass of K^* , D^+ and K^* isolation etc to remove the background. We did this by looking at the Monte Carlo plots after the pre-selection step and used values from these plots to discard the background and calculated the figure of merit (fom) using the equation 3,

$$fom = \frac{s}{\sqrt{(5 + b)}} \dots \dots \dots Equation 3$$

‘s’ is the number of Monte Carlo simulated events in W mass window of width equal to 76 to 83 GeV/c².

'b' is the number of background events of real data, in the W mass window of width equal to 76 to 83 GeV/c^2 . We used exponential fit as shown in figure 5.1 and calculated the integral value of the fit curve in the mass widow.

We used only those criteria which gave the maximum figure of merit value, as given in the table 2. Therefore, we discarded those entries which have D^+ isolation value less than 0.96 and K^* isolation value less than 0.96. We further discarded those entries which have D^+ mass is less than $1.832 \text{ GeV}/c^2$ and greater than $1.94 \text{ GeV}/c^2$.

Particle property	Limit
D^+ isolation	< 0.96
K^* isolation	< 0.96
D^+ mass	$< 1.832 \text{ GeV}/c^2$
D^+ mass	$> 1.94 \text{ GeV}/c^2$

Table 2: Shows the limit that was used on the properties of the particle to remove the background.

Chapter 4 – RESULTS AND DISCUSSION

4.1 PRE-EVENT SELECTION

Figure 4.1, 4.2 are the distributions of D^+ Mass from Monte Carlo simulated data and real data. D mass is the combined mass of $K^+ \pi^- \pi^-$. Figure 4.3-4.6 are the distributions of K^+ particle that decayed from K^* . Figure 4.7, 4.8 are the distributions of π^- particle that decayed from K^* . Figure 4.9-4.14, are the distributions of mass, momentum, position in the z-axis of the K^* . Figure 4.15-4.18 are the mass and momentum of W Mass. Figure 4.19, 4.20 are the distributions of mass K^* that is vertex fitted.

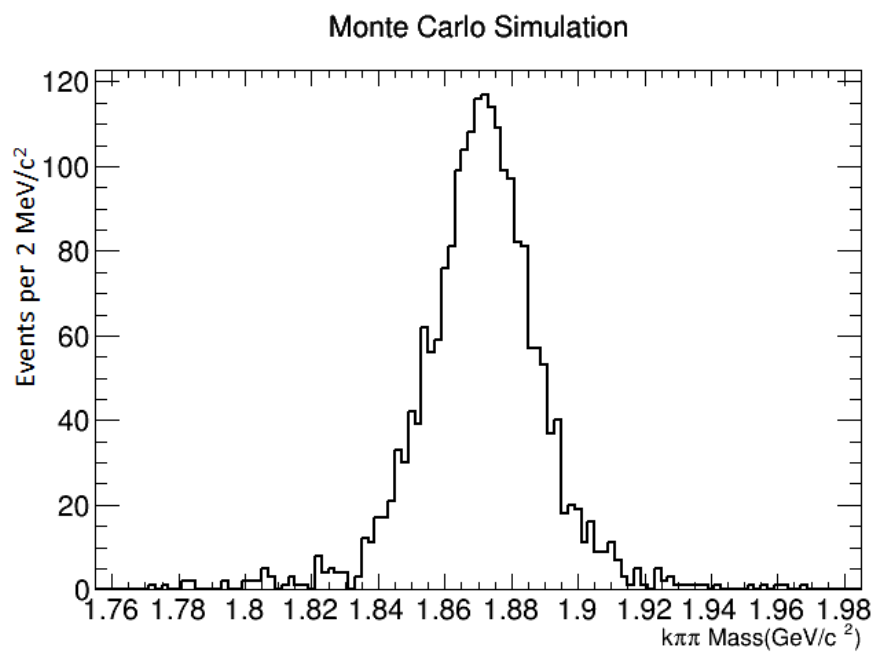


Figure 4.1: The distribution is Monte Carlo $K\pi\pi$ (D) Mass in $2 \text{ GeV}/c^2$. The y-axis is number of events per $2 \text{ MeV}/c^2$

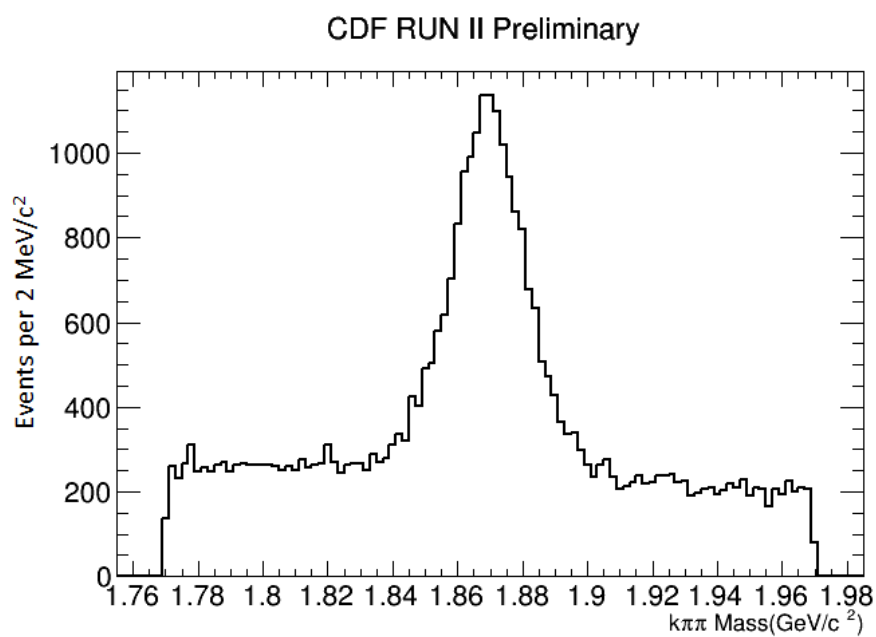


Figure 4.2: The distribution is real data, $K\pi\pi$ (D) Mass in GeV/c^2 . The y-axis is number of events per $2 \text{ MeV}/c^2$

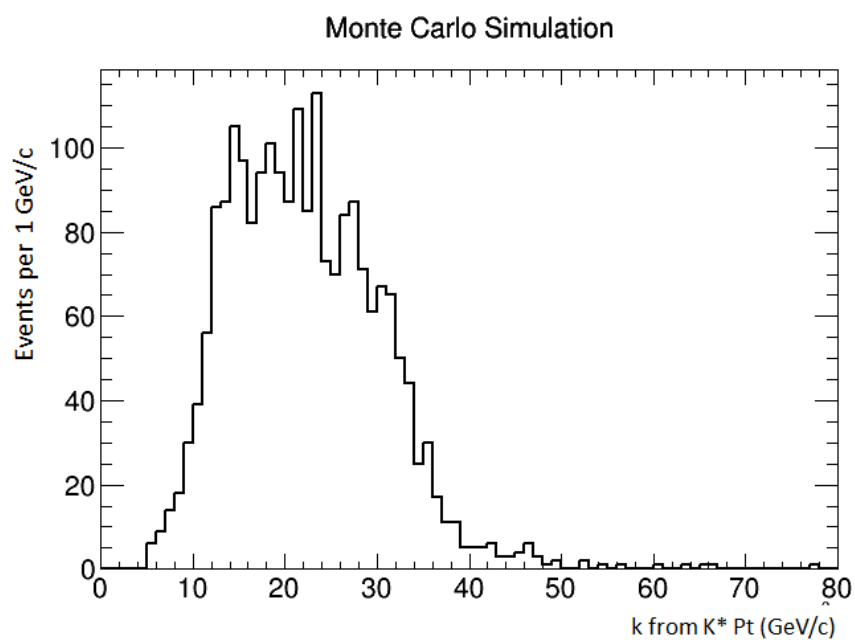


Figure 4.3: Distribution is Monte Carlo K^+ from K^* momentum in GeV/c . The y-axis is number of events per $1 \text{ GeV}/c$

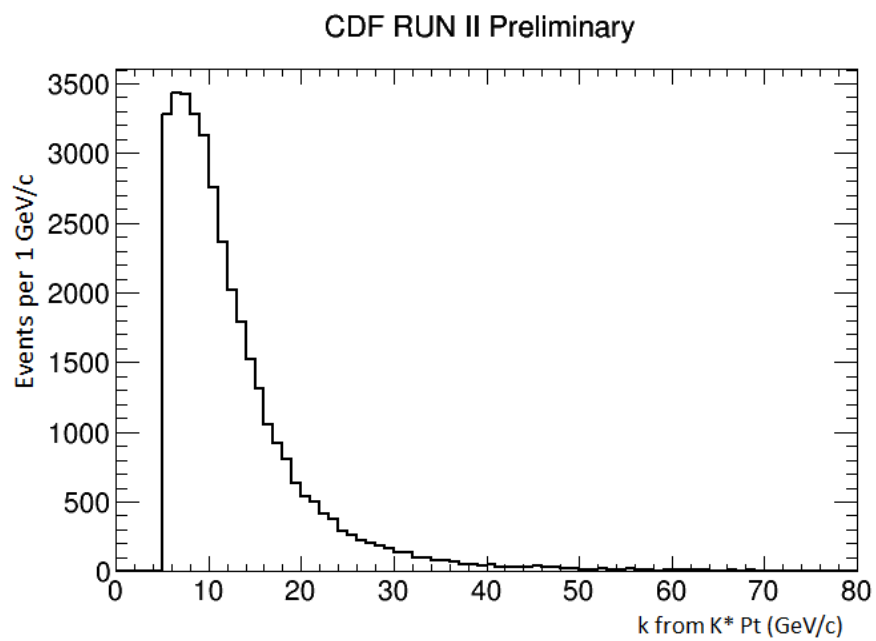


Figure 4.4: Distribution is real data, K^+ from K^* momentum in GeV/c . The y-axis is number of events per $1 \text{ GeV}/c$

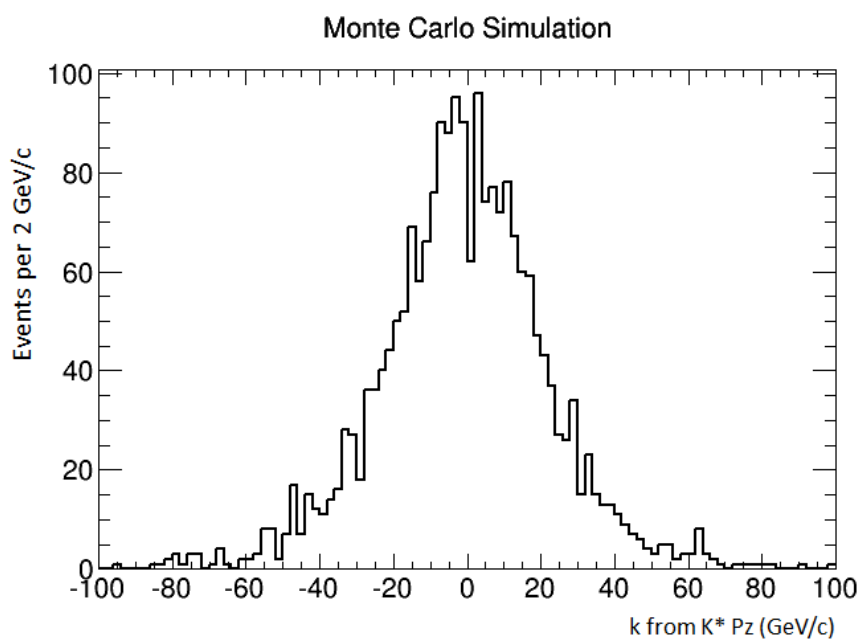


Figure 4.5: Distribution is Monte Carlo K^+ from K^* momentum in Z direction in GeV/c. The y-axis is number of events per 2 GeV/c

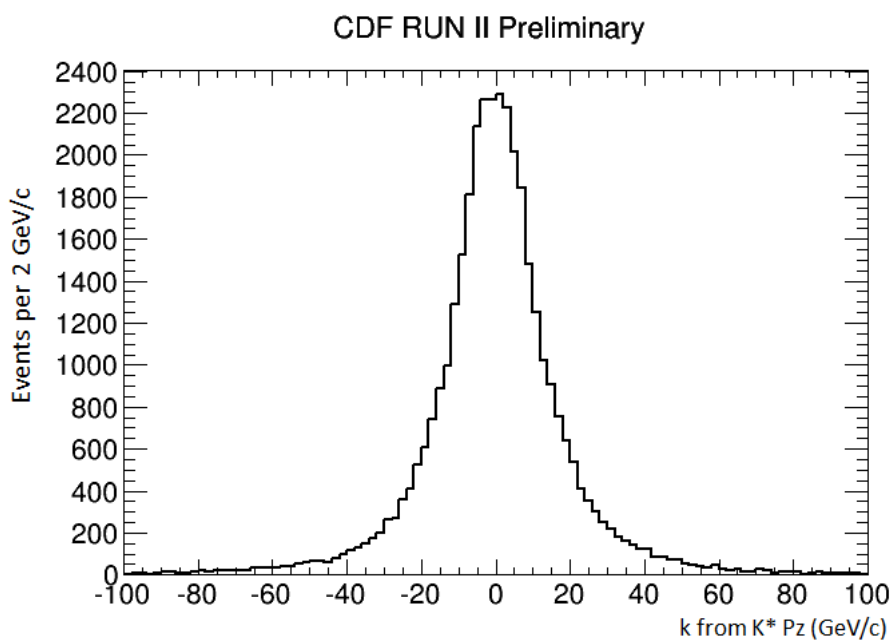


Figure 4.6: Distribution is real data, K^+ from K^* momentum in Z direction in GeV/c. The y-axis is number of events per 2 GeV/c

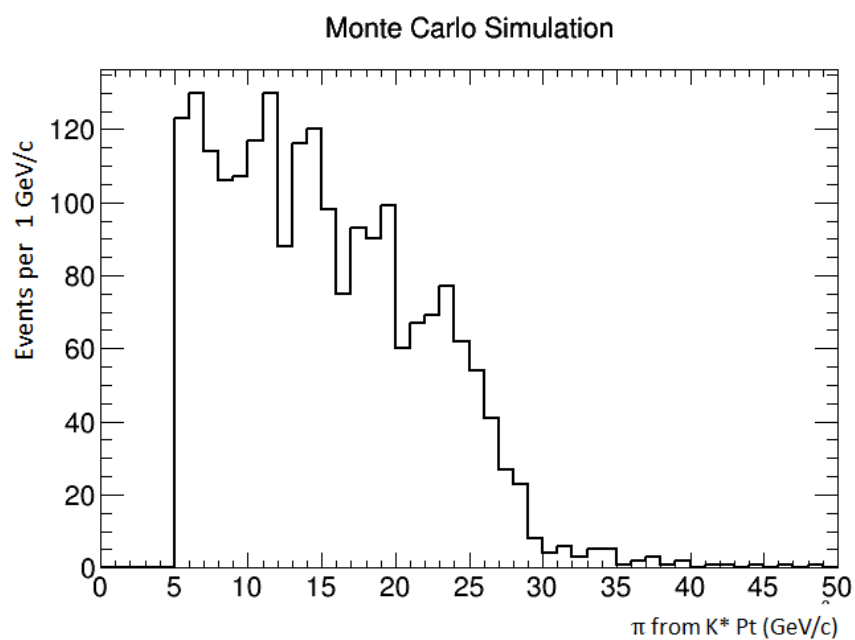


Figure 4.7: Distribution is Monte Carlo π - momentum in GeV/c. The y-axis is number of events per 1 GeV/c

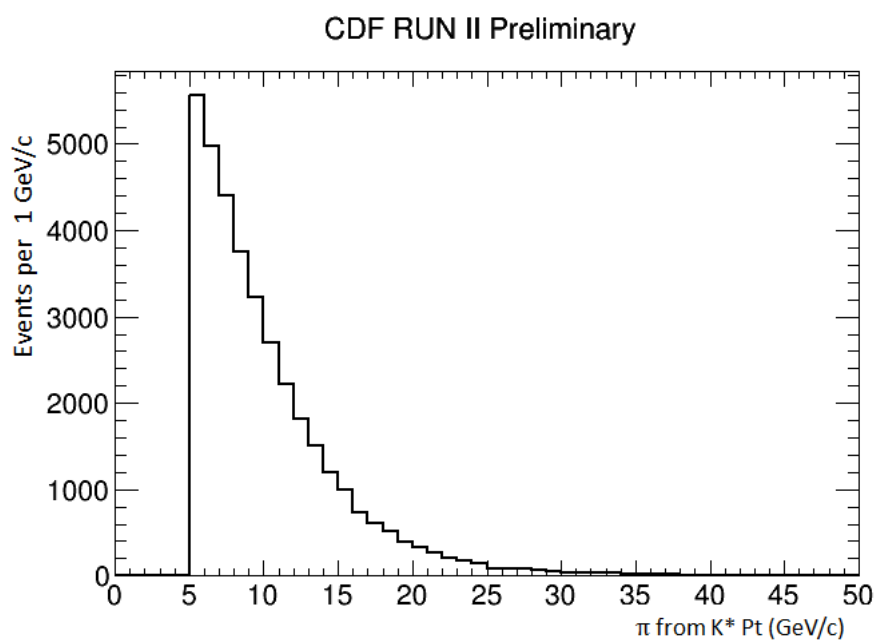


Figure 4.8: Distribution is real data, π - momentum in GeV/c. The y-axis is number of events per 1 GeV/c

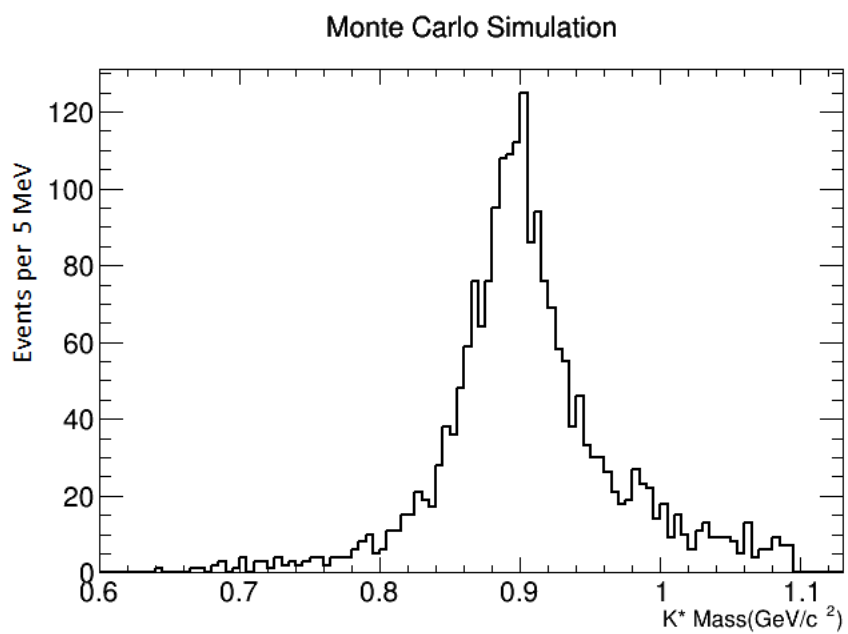


Figure 4.9: Distribution is Monte Carlo $K\pi(K^*)$ mass in GeV/c^2 . The y-axis is number of events per 5 MeV

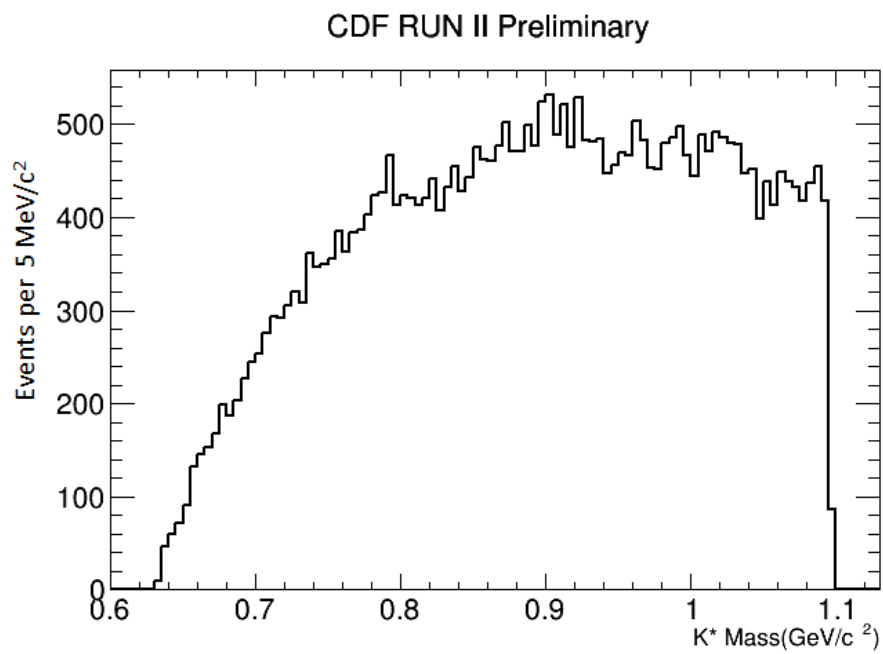


Figure 4.10: Distribution is real data, $K\pi(K^*)$ mass in GeV/c^2 . The y-axis is number of events per 5 MeV

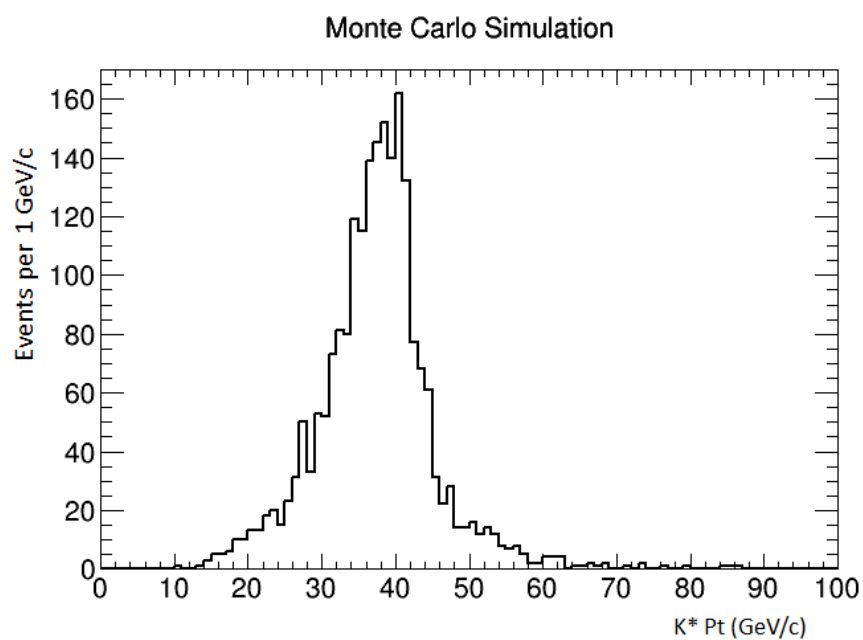


Figure 4.11: Distribution is Monte Carlo $K^* Pt$ (K^*) momentum in GeV/c. The y-axis is number of events per 1 GeV/c

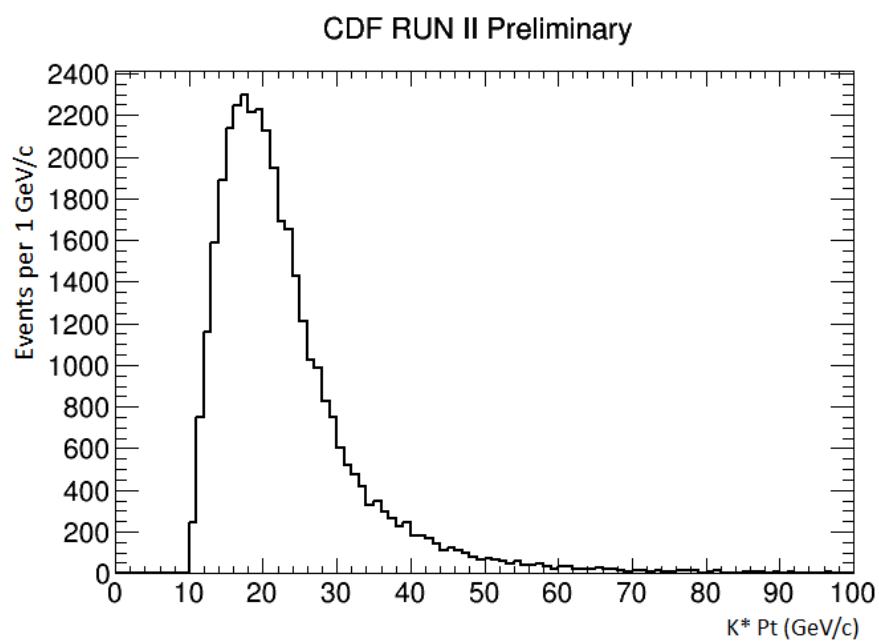


Figure 4.12: Distribution is real data, $K^* Pt$ (K^*) momentum in GeV/c. The y-axis is number of events per 1 GeV/c

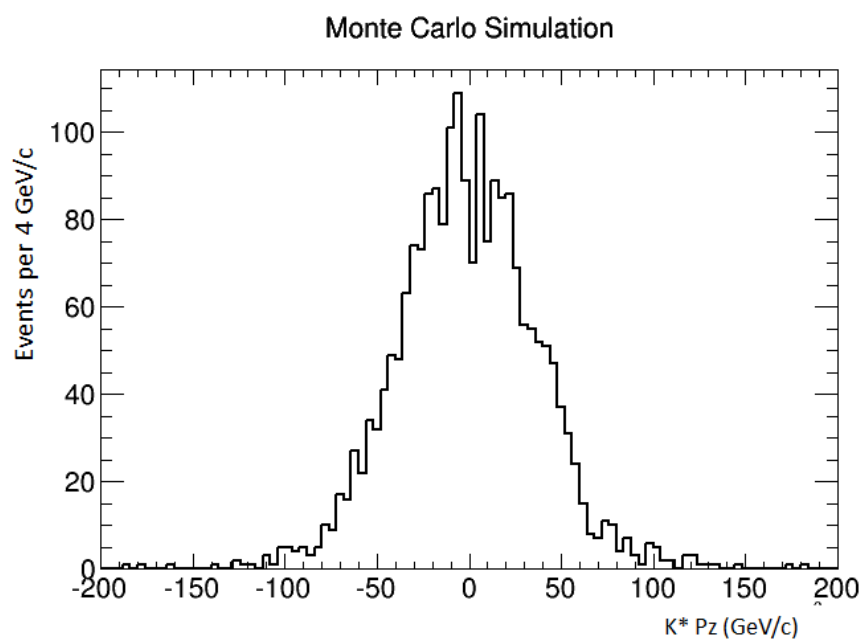


Figure 4.13: Distribution is Monte Carlo $K^* P_z$ momentum in the z direction in GeV/c. The y-axis is number of events per 4 GeV/c

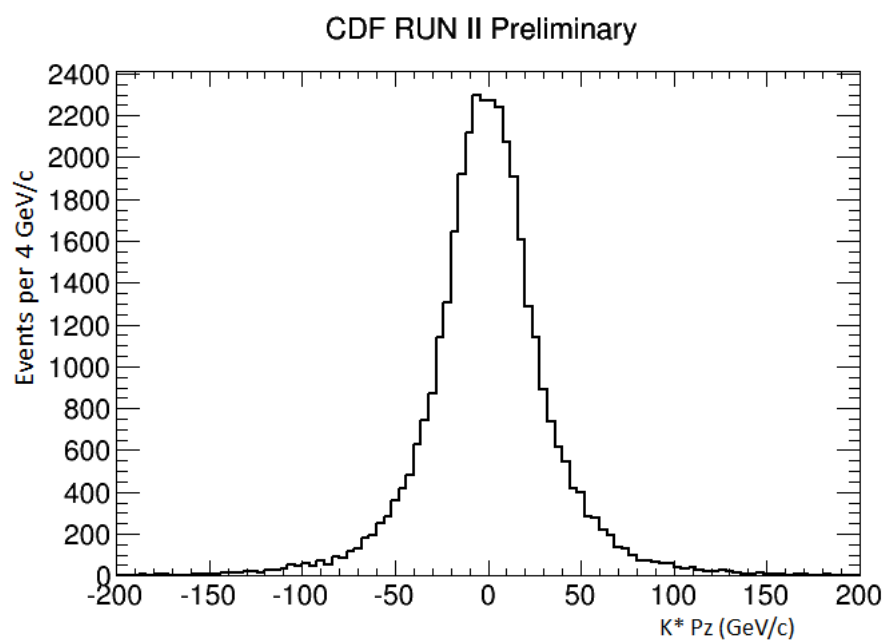


Figure 4.14: Distribution is real data, $K^* P_z$ momentum in the z direction in GeV/c. The y-axis is number of events per 4 GeV/c

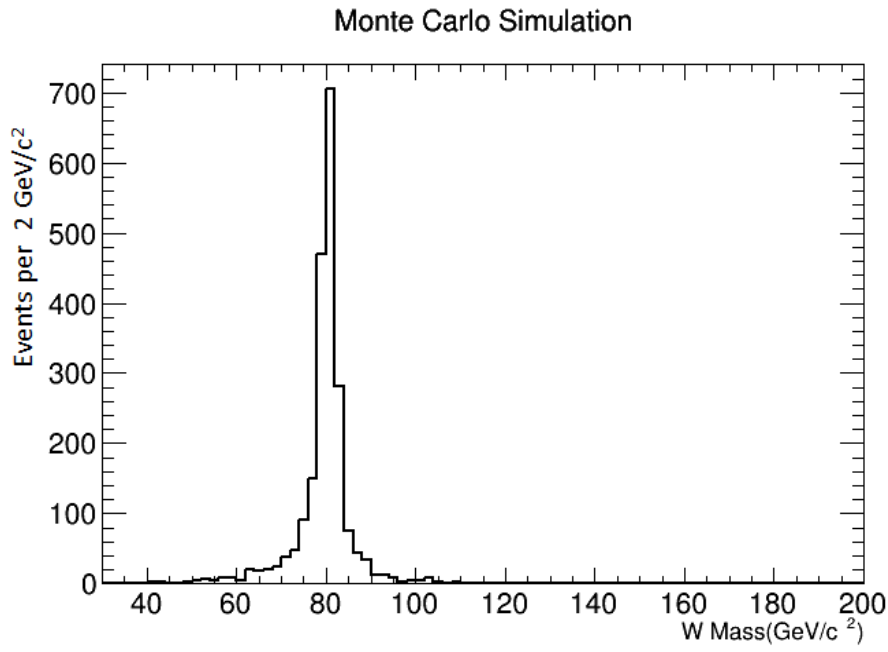


Figure 4.15: Distribution is Monte Carlo W mass GeV/c². The y-axis is number of events per 2 GeV/c²

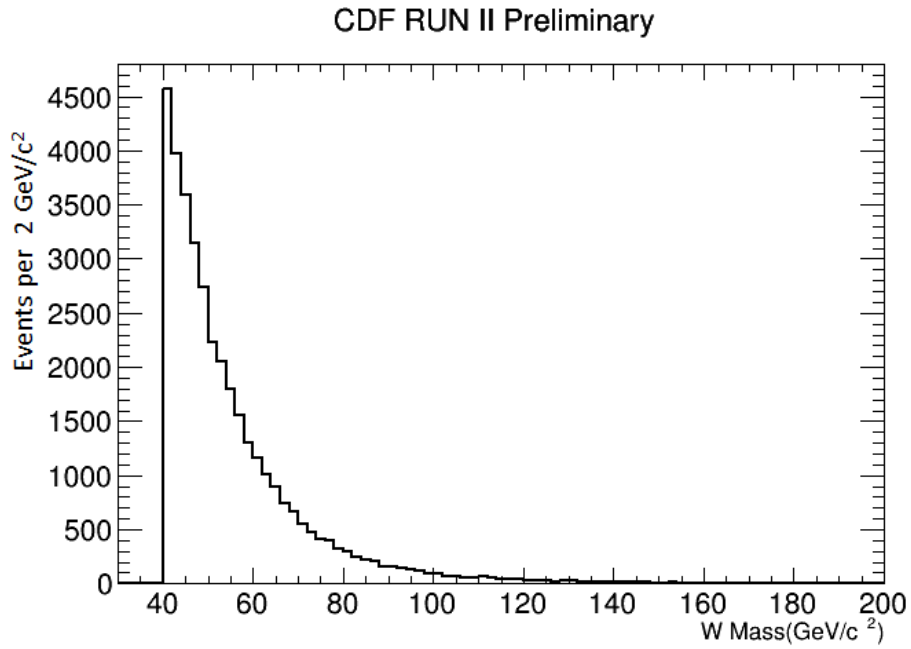


Figure 4.16: Distribution is real data W mass GeV/c². The y-axis is number of events per 2 GeV/c²

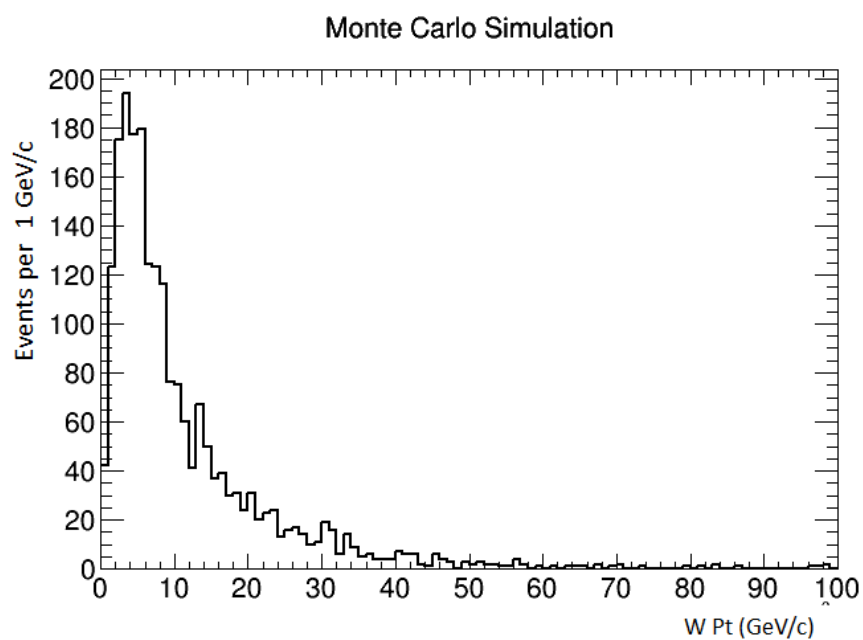


Figure 4.17: Distribution is Monte Carlo W momentum in GeV/c. The y-axis is number of events per 1 GeV/c

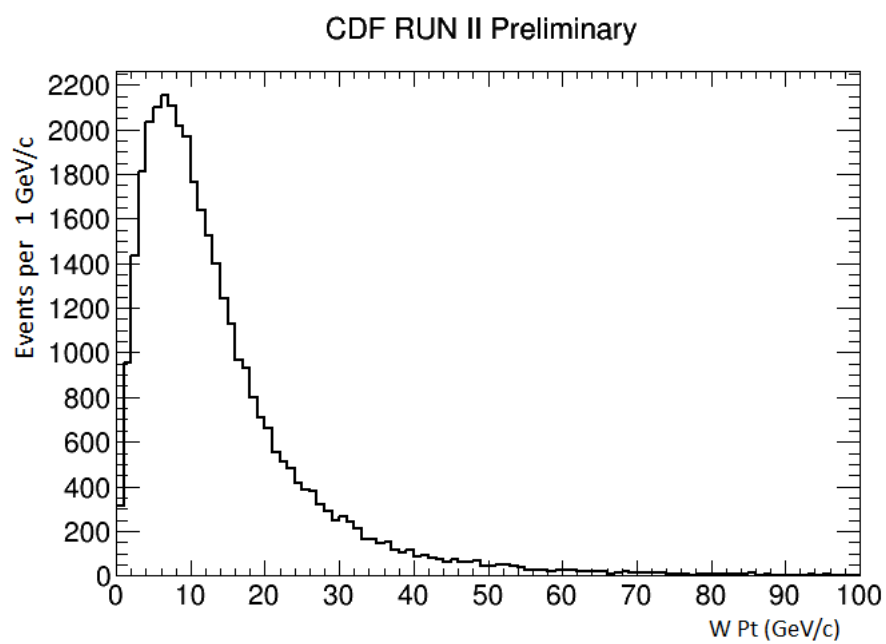


Figure 4.18: Distribution is real data W momentum in GeV/c. The y-axis is number of events per 1 GeV/c

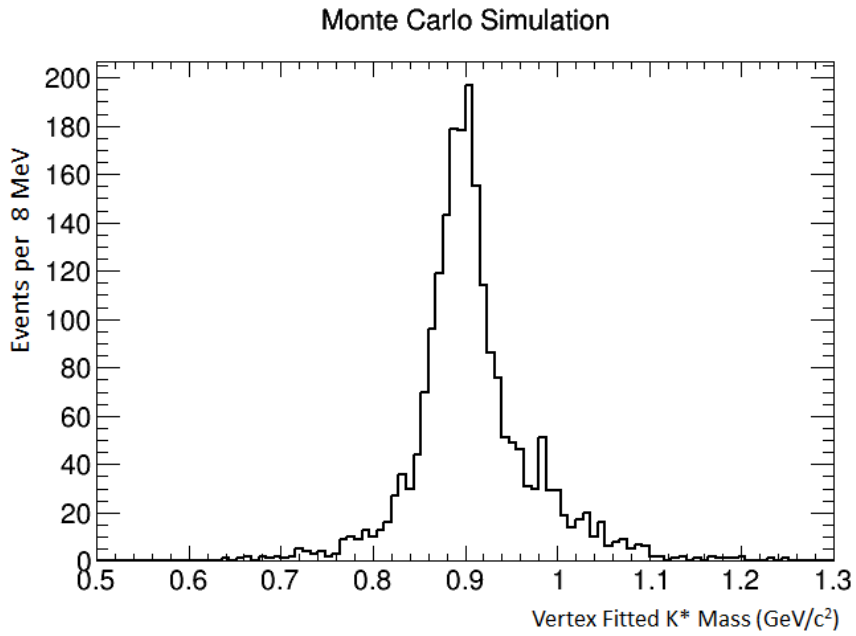


Figure 4.19: Distribution is Monte Carlo, Vertex Fitted K^* mass in GeV/c^2 . The y-axis is number of events per 8 MeV.

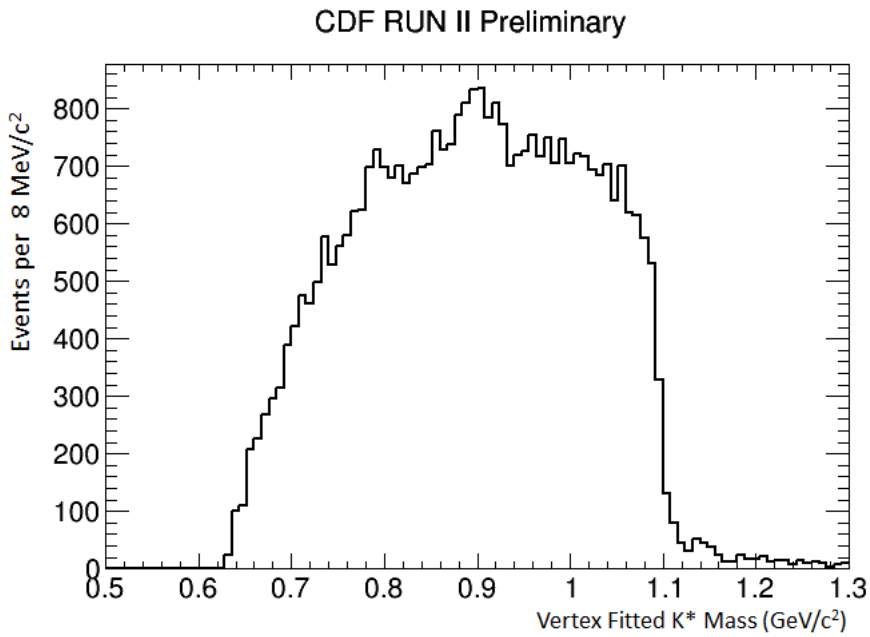


Figure 4.20: Distribution is real data, Vertex Fitted K^* mass in GeV/c^2 . The y-axis is number of events per 8 MeV.

4.2 EVENT SELECTION

Figure 4.21 and 4.22 are Monte Carlo and real data distributions of $K\pi\pi$ (D^+) isolation, showing the vertical line on the plot as the position of selection cuts made to filter the background. Figure 4.23, 4.24 are Monte Carlo and real data distributions of K^* isolation, showing the vertical line as the position of selection cuts. Figure 4.25, 4.26 are Monte Carlo and real data distribution of D^+ mass, showing the vertical line as the position of selection cuts.

Figure 4.27, 4.28 are Monte Carlo and real data distributions of $K\pi\pi$ mass in GeV/c^2 after selection cuts. Figure 4.29, 4.30 are Monte Carlo and real data distribution of the W mass in GeV/c^2 after selection. Figure 4.31 is real data 3D distribution of $K\pi\pi$ mass and W Mass in GeV/c^2 after selection

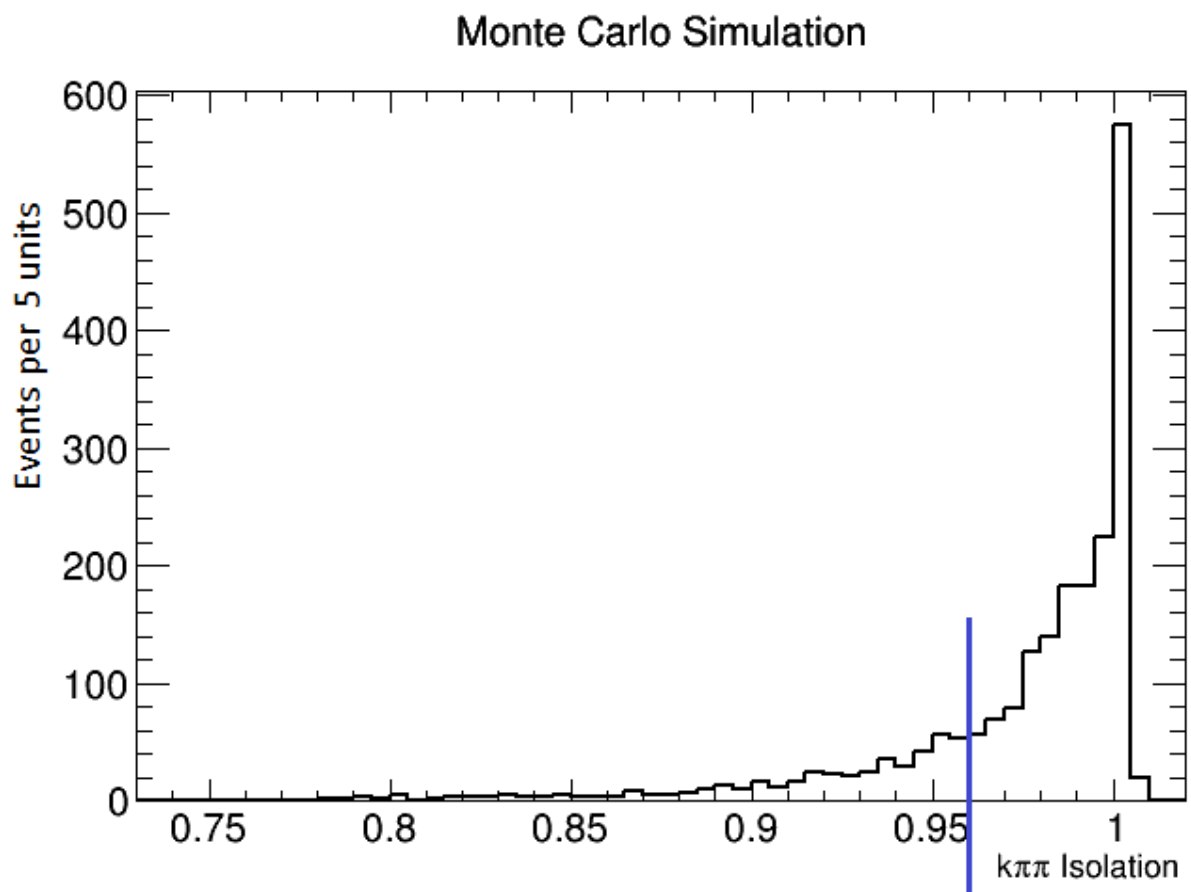


Figure 4.21: Distribution is Monte Carlo $K\pi\pi$ (D^+) isolation. Y axis is the number of events per 5 units. Vertical line on the plot is the cut made in the selection process in the step 2.

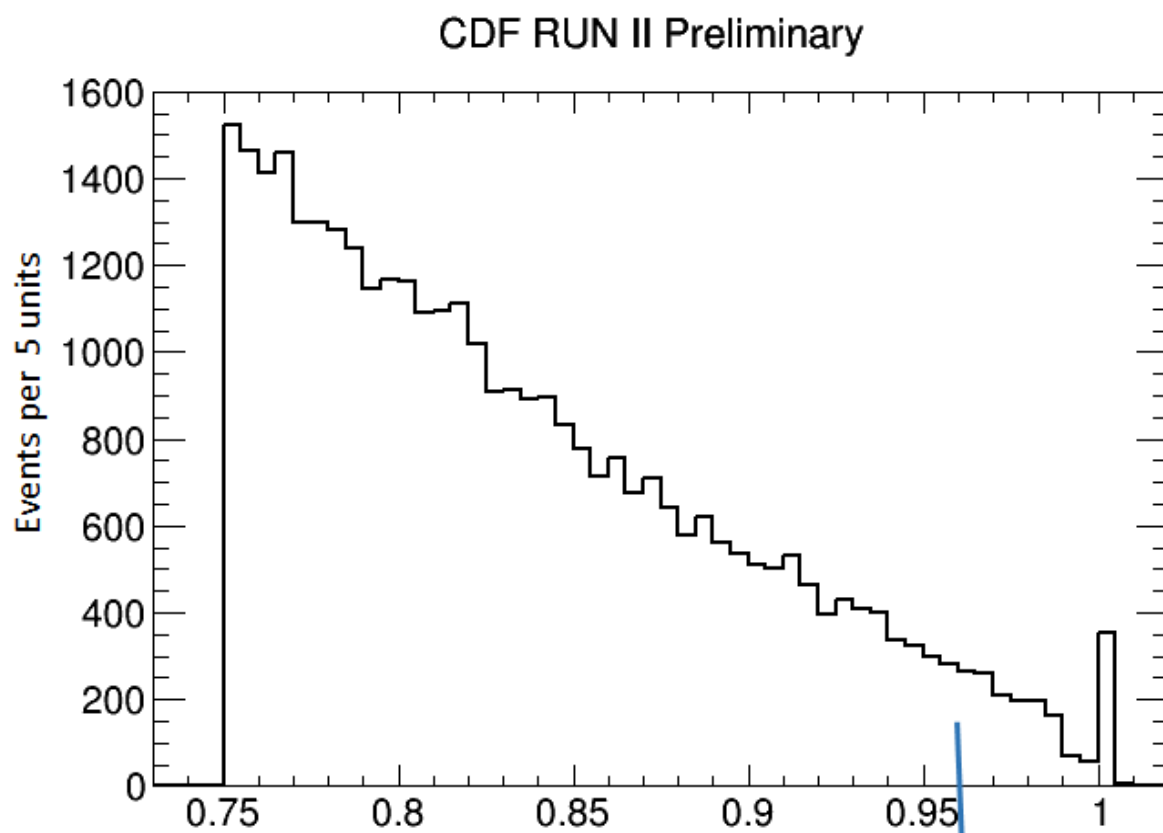


Figure 4.22: Distribution is real data $K\pi\pi$ (D^+) isolation. Y axis is number of events per 5 units. Vertical line on the plot is the cut made in selection process in the step 2

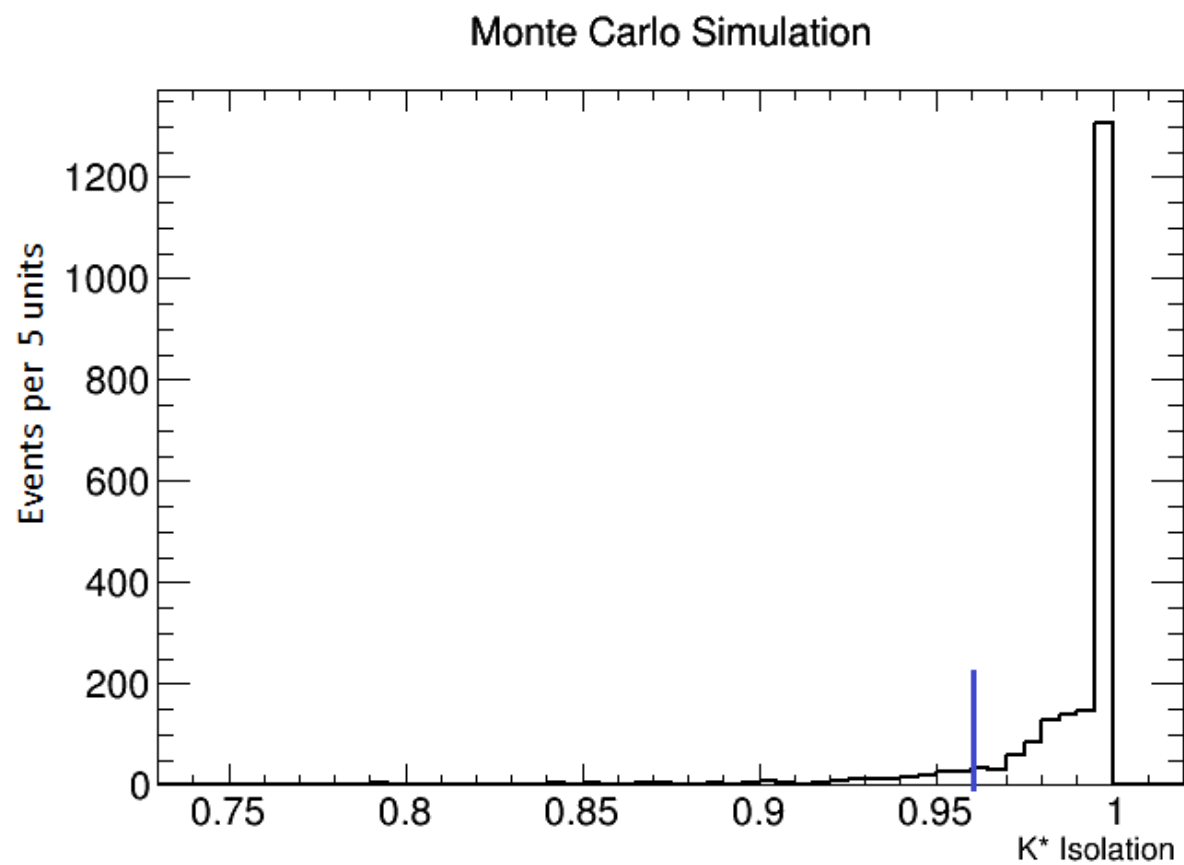


Figure 4.23: Distribution is Monte Carlo K^* isolation. Y axis is the number of events per 5 units. Vertical line on the plot is the cut made in the selection process in the step 2.

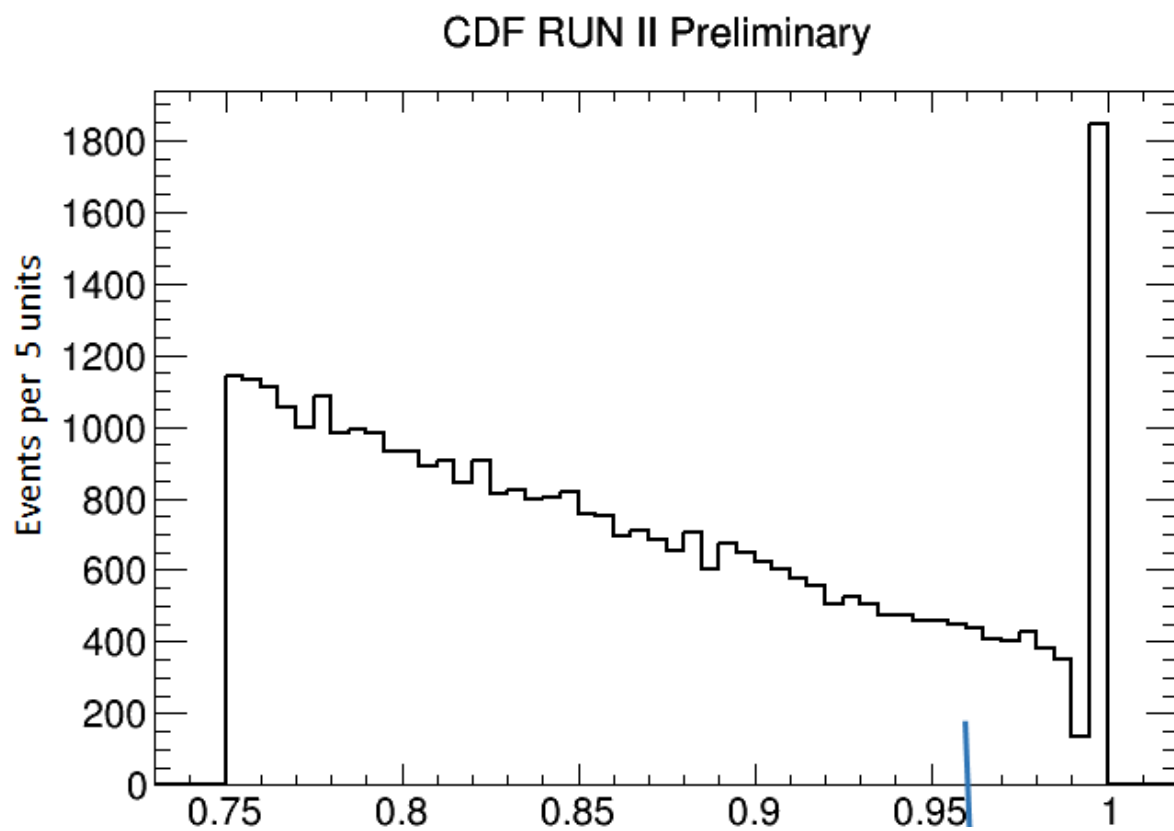


Figure 4.24: Distribution is real data K^* isolation. Y axis is number of events per 5 units. Vertical line on the plot is the cut made in selection process in the step 2.

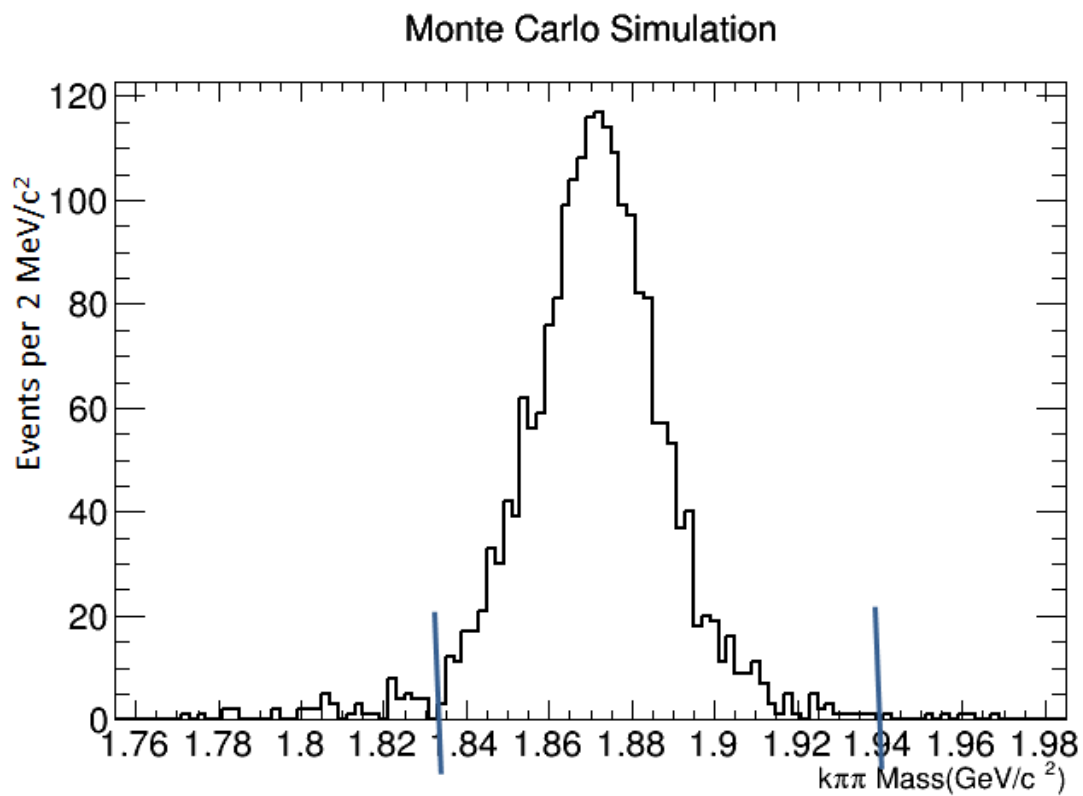


Figure 4.25: Distribution is Monte Carlo KPiPi (D^+) Mass. Y axis is the number of events per 2 MeV/c². Vertical line on the plot is the cut made in the selection process in the step 2.

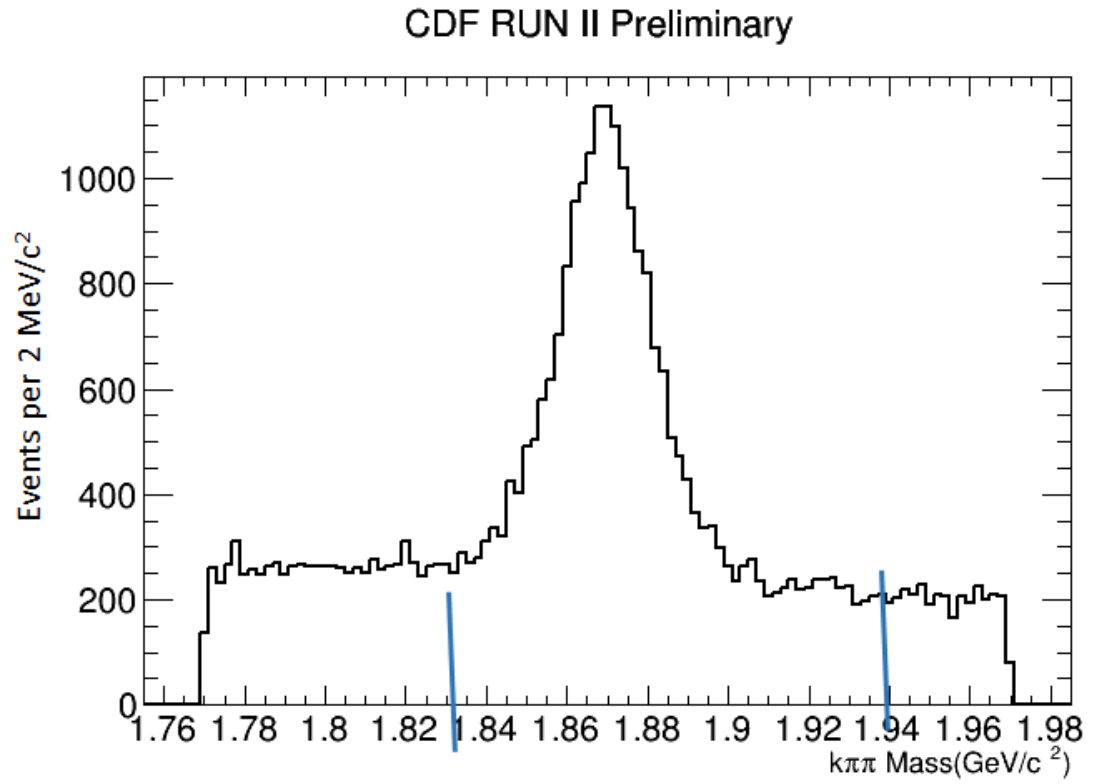


Figure 4.26: Distribution is real data $K\pi\pi$ (D^+) Mass. Y axis is the number of events per $2 \text{ MeV}/c^2$. Vertical line on the plot is the cut made in the selection process in the step 2.

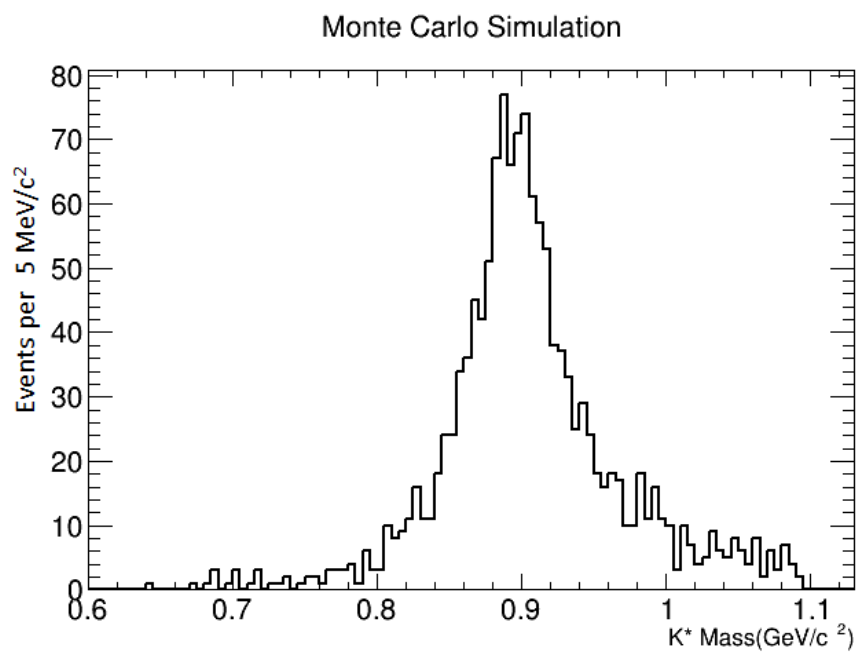


Figure 4.27: Distribution is Monte Carlo K^* mass in GeV/c^2 after selection. The y-axis is number of events per $5 \text{ MeV}/c^2$

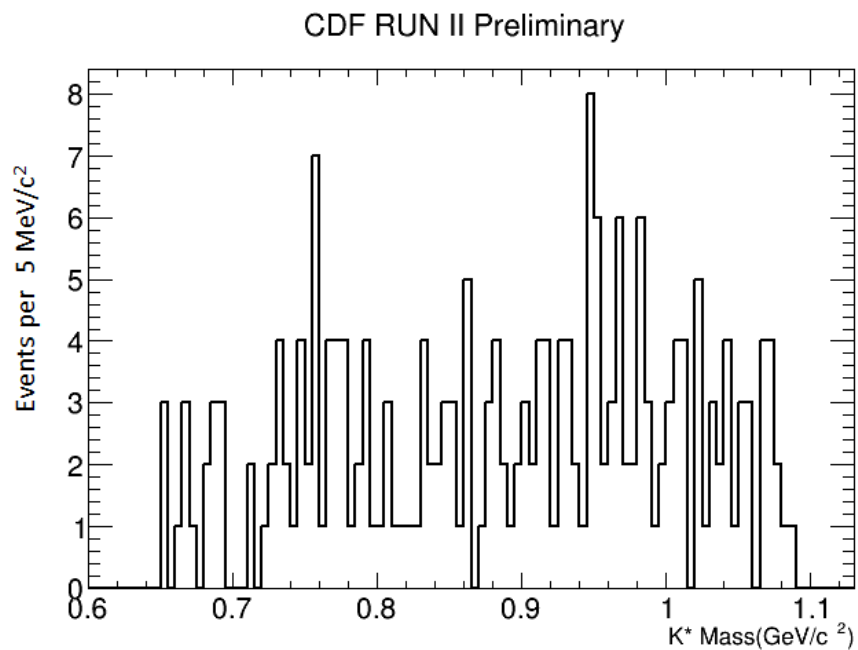


Figure 4.28: Distribution is real data, K^* mass in GeV/c^2 after selection. The y-axis is number of events per $5 \text{ MeV}/c^2$

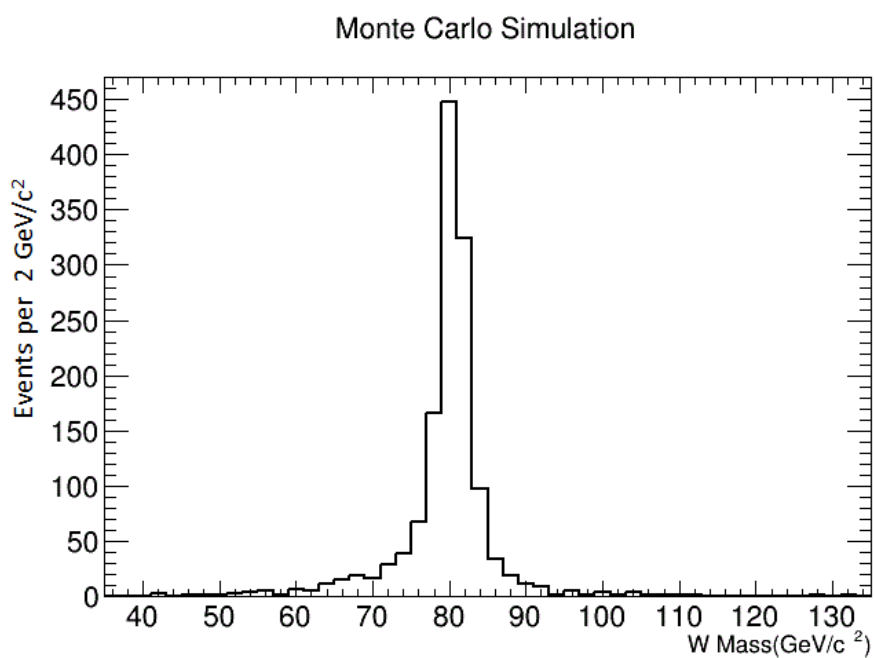


Figure 4.29: Distribution is Monte Carlo, W mass in GeV/c^2 after selection. The y-axis is number of events per $2 \text{ GeV}/c^2$

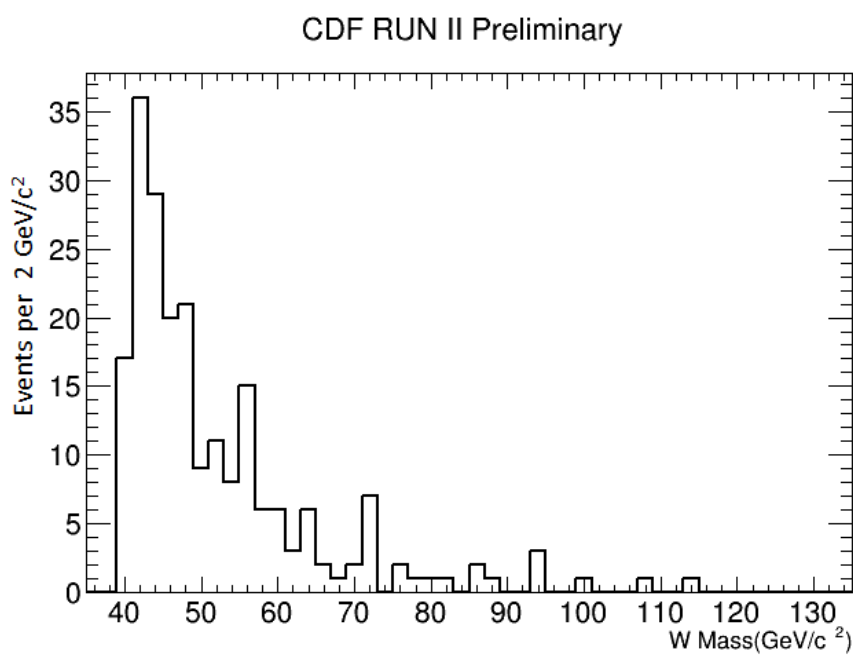


Figure 4.30: Distribution is real data, W mass in GeV/c^2 after selection. The y-axis is number of events per $2 \text{ GeV}/c^2$

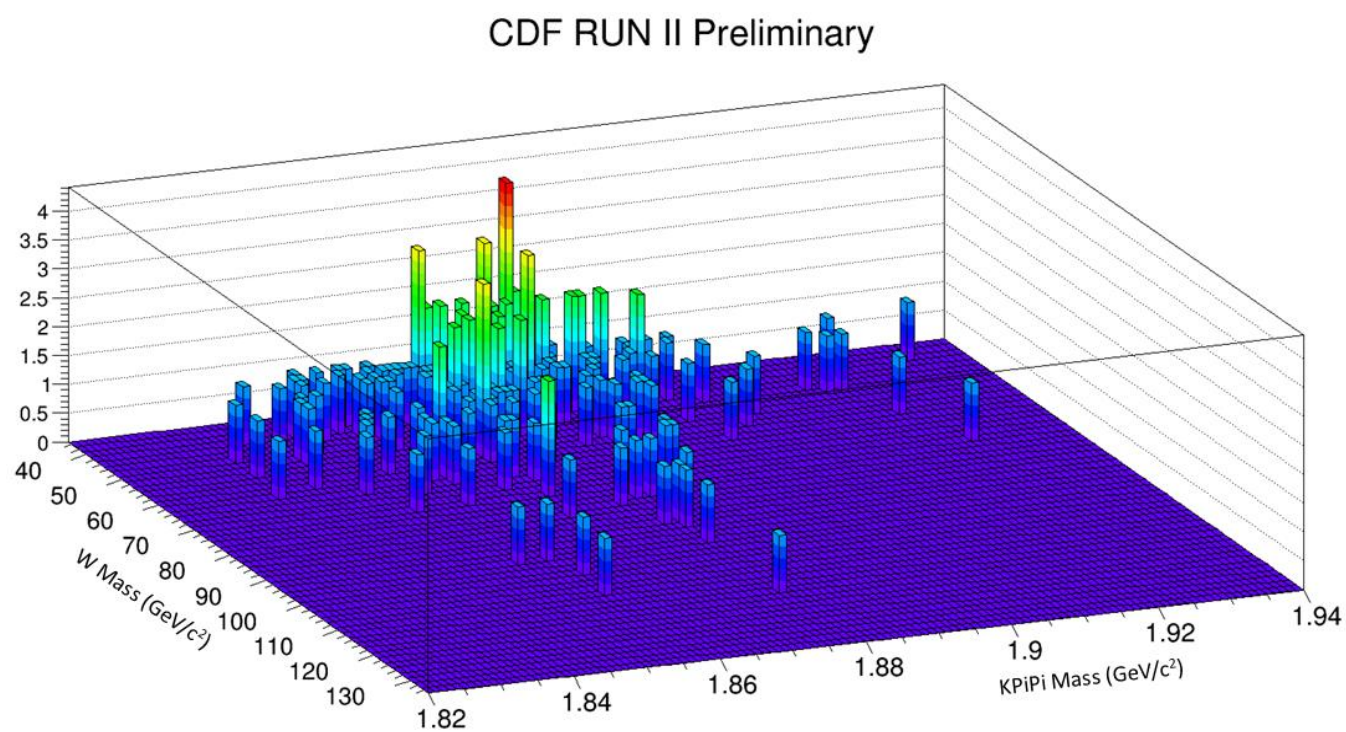


Figure 4.31: 3D Distribution is real data, KPiPi mass and W Mass in GeV/c^2 after selection.

CHAPTER 5 – CONCLUSION

We report on the investigation of hadronisation decay mode of the W boson. We looked for the decay modes of $W \rightarrow D^+ K^*$, with D^+ and K^* decaying as, $D^+ \rightarrow K^- \pi^+ \pi^+$ and $K^* \rightarrow K^+ \pi^-$. Figure 4.26 and Figure 4.27 shows the distribution of the W mass after the pre-selection and the selection steps. We did an exponential fit on W Mass distribution of real data to separate the signal and background as seen in the Figure 5.1.

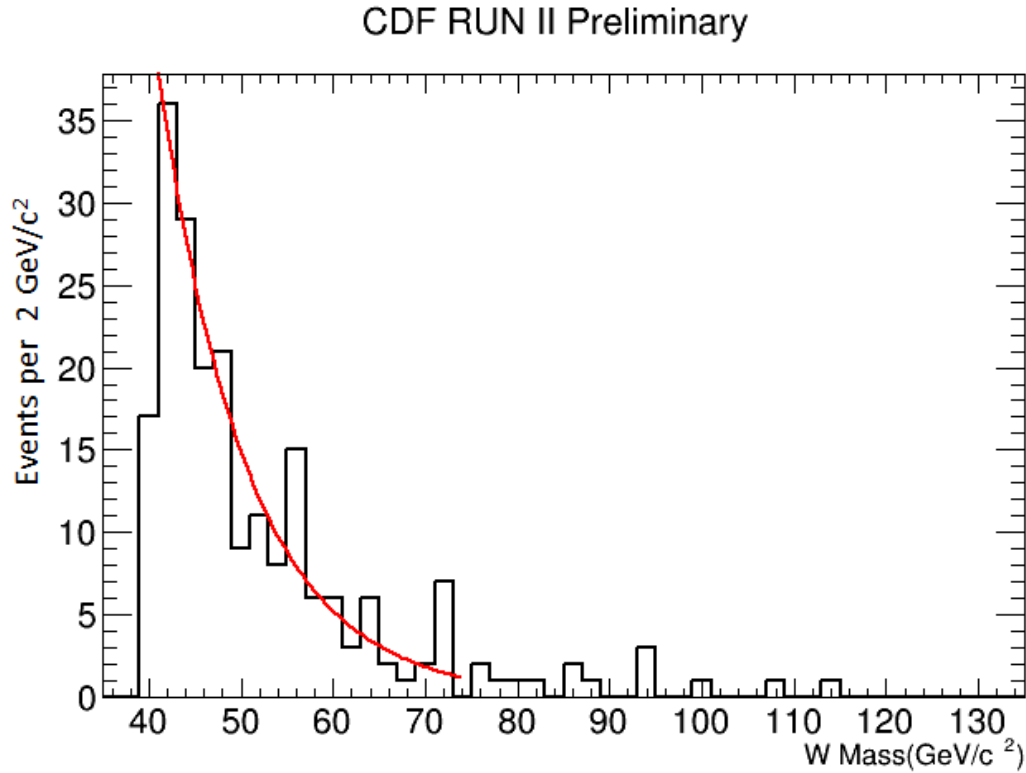


Figure 5.1: Exponential fit of W Mass.

We calculated branching fraction of this decay mode using the equation 4 and found the values to be,

$$B_W < \frac{N_{WDK^*}}{N_W * B_D * B_{K^*} * e} = 7.99 * 10^{-6} \dots\dots\dots \text{Equation 4}$$

B_W , Branching fraction of $W \rightarrow D^+ K^*$.

N_{WDK^*} , is the number of W boson produced, with decay mode, $W \rightarrow D^+ K^*$ and its value is 10.29. We got this value from the Table 1V of [11] using the number of signal events, n_0 and the number of background signal events, b in the mass window width of 76 - 83 GeV/c² of the W mass real data distribution with exponential fit. To calculate background, b , we used exponential fit and calculated the integral value of the fit curve in the mass widow.

N_W , Number of W boson produced, Integrated Luminosity (nb⁻¹)*Cross Section (pb), 2.16*10⁸.

B_D , Branching fraction of $D^+ \rightarrow K^- \pi^+ \pi^+$, 0.0913 [10].

B_{K^*} , Branching fraction of $K^* \rightarrow K^+ \pi^-$, 0.67 [10].

e , efficiency for signal, $e = \frac{s}{N}$; s , is the number of Monte Carlo simulated events in mass window of width equal to 76 to 83 GeV/c² and its value is 0.0975. N is the total number of signals generated.

BIBLIOGRAPHY

1. <http://home.web.cern.ch/about/physics/standard-model>][<http://physics.info/standard/>]
[1].
2. Glashow (1967) [2].
3. The Mass and Width of the W boson, MWGrunewald,A.Gurtu [3].
4. <http://www.fnal.gov/pub/tevatron/>[4].
5. Fig: Aerial view of the Fermilab rings, Copied from
<http://www.fnal.gov/pub/presspass/images/sigma-b-baryon-images.html> [5].
6. http://www-bdnew.fnal.gov/operations/rookie_books/Concepts_v3.6.pdf [6].
7. <http://www-cdf.fnal.gov/upgrades/tdr/tdr.html> [7].
8. http://www-cdf.fnal.gov/upgrades/silicon/Introduction_Goals.html#fig:cdfiitracking
[8].
9. The CDF II Detector Technical Design Report FERMILAB-Pub-96/390-E ,computing and
software[9]
10. REVIEW OF PARTICLE PHYSICS, 2012 [11].

ABSTRACT**SEARCH FOR FULLY RECONSTRUCTED W BOSON DECAY**

by

SANGEETHA BASKARAN**MAY 2015****Advisor:** Dr. Robert Harr**Major:** Physics**Degree:** Master of Science

We have applied techniques used in reconstructing charm and bottom hadron decays to reconstruct W boson decay. This technique can also be used for the study of other heavy boson decays. We search for the decay of a W boson to a D^+ meson and a K^{*0} meson. Events are selected based on the topology of the displaced decay vertex of the $D^+ \rightarrow K^- \pi^+ \pi^+$. The K^{*0} is reconstructed in its $K^\pm \pi^\mp$ decay mode.

AUTOBIOGRAPHICAL STATEMENT

Sangeetha Baskaran was born June 6, 1983, Chennai, Tamil Nadu, India to Usha Baskaran and Baskaran Natarajan. She lived and did her schooling in Chennai, Bangalore and Delhi, India and finally completed her high school education in May, 2001. She then pursued her undergraduate studies receiving a Bachelor of Engineering from Santhosha Engineering College (Anna University), Chennai in May, 2005 specializing in Information Technology.

She was a Software Trainee at the Polaris Financial Technology Limited, Chennai, India, from January 2005 to May 2005. She then worked as a Software Engineer in OptimusBT, Bangalore, India, from January 2006 to September 2007. She then joined Verizon Data Services India, Chennai as a Software Engineer and got promoted as an Analyst. She was then married to Arvind Govindaraj on April 18th, 2010 and moved to US with her husband. For the passion for science, she wanted to pursue higher studies in physics. She got accepted at Wayne State University, Detroit to the Master's program in physics for the fall 2012. Her hope is to work in a vibrant, technologically challenging and creative roles. She also wants to put the use of her education and understanding of science to a good cause.